Palaeogeography, Palaeoclimatology, Palaeoecology 699 (2026) 114023

Contents lists available at ScienceDirect

Palaeogeography, Palaeoclimatology, Palaeoecology

journal homepage: www.elsevier.com/locate/palaeo

Quantitative analysis of Upper Miocene Mediterranean reef carbonates: A tool for reconstructing palaeoenvironmental gradients☆

Giovanni Coletti[a,*], Alberto Vimercati[a], Francesca R. Bosellini[b], Luca Mariani[b], Adriano Guido[c], Alessandro Vescogni[b], Jesús Reolid[d], Gerald Auer[e], Daniela Basso[a], Alberto Collareta[f], Giulia Bosio[a,f], Or Mordecai Bialik[g,h]

[a] Dipartimento di Scienze dell'Ambiente e della Terra, Università degli Studi di Milano-Bicocca, 20126 Milano, Italy
[b] Dipartimento di Scienze Chimiche e Geologiche, Università di Modena e Reggio Emilia, Via Campi 103, I-41125, Italy
[c] Department of Biology, Ecology and Earth Sciences, University of Calabria, Via Bucci, cubo 15b, 87036 Rende, Cosenza, Italy
[d] Departamento de Estratigrafía y Paleontología, Universidad de Granada, Avenida Fuentenueva s/n, 18071 Granada, Spain
[e] University of Graz, Department of Earth Sciences, NAWI Graz Geocenter, Heinrichstrasse 26, 8010 Graz, Austria
[f] Dipartimento di Scienze della Terra, Università di Pisa, 56126 Pisa, Italy
[g] Institute of Geology and Paleontology, University of Münster, Corrensstr. 24, 48149 Münster, Germany
[h] Israel Oceanographic and Limnological Research, National Institute of Oceanography, Haifa 310800, Israel

ARTICLE INFO

Editor: Professor L Angiolini

Keywords:
Reef
Corals
Benthic foraminifera
Messinian
Tortonian
Carbonate Factory

ABSTRACT

During latest Miocene times the Mediterranean Sea main connection with the global ocean was through the Atlantic, just as it is today. This configuration could have likely resulted in a pronounced longitudinal environmental gradient, with warm and highly oligotrophic waters in the east, and cooler, less oligotrophic conditions in the west (a scenario resembling modern conditions). This setting provides a natural laboratory to test the effectiveness of quantitative microfacies analysis in tracking palaeoenvironmental gradients. Two approaches were compared: the presence/absence of carbonate producers assessed on the basis of literature data and a quantitative skeletal assemblage analysis of reef sites spanning the Western, Central, and Eastern Mediterranean. While the presence/absence approach only offers a broad environmental overview, the quantitative analysis better differentiates between the eastern and western settings. The eastern sector displays a higher relevance of symbiont-bearing foraminifera, suggesting warmer conditions. In contrast, the western sector is comparatively richer in heterotrophic organisms, likely reflecting a higher nutrient availability and cooler water. These results support the reliability of quantitative microfacies analysis and provide a framework for comparing reef-bearing, carbonate systems across the Mediterranean within climatic homogeneous time intervals. Both approaches suggest that these carbonate factories represent subtropical, modern-like, biotic assemblages adapted to the cooler, oligotrophic, and likely semi-restricted conditions that were prevalent prior to the Messinian Salinity Crisis.

1. Introduction

Tracking environmental gradients on the long time scale (>10^3 years) is challenging due to the relevance of evolutionary processes and the effects of the complex feedback mechanisms between the biosphere, atmosphere, hydrosphere, and geosphere (Ridgwell and Zeebe, 2005; Pomar et al., 2017). Due to their preservation potential, fossil skeletal assemblages of invertebrate carbonate producers can provide valuable insights into long-term environmental trends, but the information they provide is generally constrained by the limits of temporal resolution. However, what they lack in accuracy can often be compensated for by the quantity of data, as fossil occurrences of biogenic carbonates are widespread. Using a large set of samples from different localities can help in reducing background noise and capturing environmental processes at large spatial and temporal scales (Kiessling et al., 1999; Aguirre et al., 2000; Flügel and Kiessling, 2002; Bosellini and Perrin, 2008;

☆ This article is part of a Special issue entitled: 'Mediterranean Miocene' published in Palaeogeography, Palaeoclimatology, Palaeoecology.

* Corresponding author.
E-mail address: giovanni.coletti@unimib.it (G. Coletti).

https://doi.org/10.1016/j.palaeo.2026.114023
Received 1 December 2025; Received in revised form 20 June 2026; Accepted 26 June 2026
Available online 28 June 2026

Johnson et al., 2008; Coletti et al., 2018, 2022; Benedetti et al., 2024; Agiadi et al., 2024a, 2024b; Bosellini et al., 2025).

So far attempts at analysing large-scale past environmental variability using fossil skeletal assemblages have primarily relied on presence/absence data (e.g., Kiessling et al., 1999) and taxonomic richness datasets (e.g., Agiadi et al., 2024a, 2024b). Presence/absence dataset (or frequency of reported occurrences) can highlight major shifts in time and space (e.g., crises or extinctions of certain groups; Flügel and Kiessling, 2002). Since these "boolean datasets" significantly reduce the complexity of the information to a binary option (presence/absence), they can easily integrate data from multiple sources (e.g., field guidebooks, detailed analyses in academic papers, and technical reports). Analyses of taxonomic richness can be considered as a more informative type of presence/absence dataset, but their creation is significantly more time-consuming (Agiadi et al., 2024a, 2024b). Furthermore, they are limited by the ability to correctly recognize a type of organism, and, thus, they are often restricted to a single taxonomic group (e.g., Benedetti et al., 2024; Bosellini et al., 2025). An abundance-based approach to the study of fossil carbonate producers has been attempted for the analysis of microfacies and in particular in stratigraphic studies (e.g., Brandano et al., 2009; Guido et al., 2016, 2021; Mariani et al., 2024, 2026). This methodology could be useful in investigating large-scale environmental variability, and because microfacies investigations often focus on higher taxonomic levels (families, classes or above), taxonomic complexity is less of a problem.

To test the quantitative microfacies approach, we investigated the potentially strong environmental gradient that existed in the Late Miocene Mediterranean Sea before the Messinian Salinity Crisis (MSC). We hypothesize, based on palaeoceanographic constraints (e.g., Capella et al., 2019), that during the Late Miocene the environmental gradient should roughly mirror the current condition, i.e., a slightly colder, less oligotrophic, and less saline surficial water mass to the west and a warmer, more oligotrophic, and saline one to the east (Antoine et al., 1995; Bosc et al., 2004; Pastor et al., 2019). We then reviewed existing information on particularly sensitive environments: coral-reefs and closely associated habitats (lagoons, fore-reefs) (e.g. Pandolfi and Kiessling, 2014). During the Late Miocene, the Mediterranean was indeed rich in coral-reefs (Bosellini and Perrin, 2008; Perrin and Bosellini, 2012), providing us with an extensive record of palaeoenvironmental information (Fig. 1). Consistently, Upper Miocene, reef-bearing, shallow-water carbonate systems from the eastern, central, and western parts of the Mediterranean were reviewed, assessing the distribution of the major carbonate-producing organisms, using both a presence/absence and a quantitative analysis (Fig. 1). The datasets were used to highlight similarities and differences between Upper Miocene and modern tropical systems, providing a more detailed picture of shallow-water tropical carbonate systems towards the end of the last major chapter of the tropical history of the Mediterranean Sea.

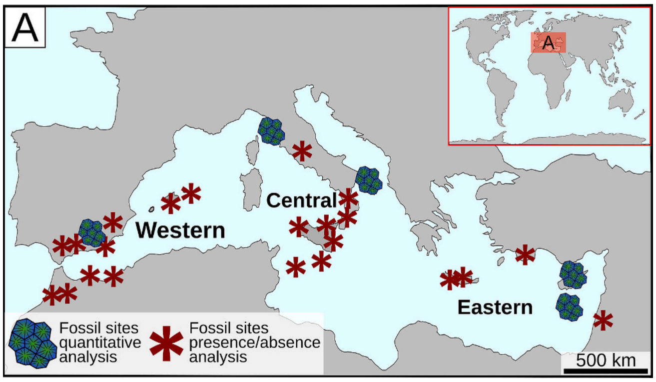

Fig. 1. Map of the Mediterranean Basin indicating the position of the sites investigated for the presence/absence analysis (for detailed coordinates of these fossil sites, see Supplementary Table S1) and those of the sites investigated for the quantitative microfacies analysis. The number of symbols for the presence absence analysis do not match the number of sites since several sites are too close to be represented separately in the figure. The inset panel indicates the panel's position in world map.

2. Methods

2.1. Background and methodological framework

Testing the potential of quantitative microfacies analysis requires the investigated geological successions to be reasonably coeval and to represent comparable environmental conditions. Meeting these requirements is a challenge in shallow-water carbonates, particularly in the Upper Miocene of the Mediterranean (e.g., Guerra-Merchán and Serrano, 1993). Shallow-marine deposits frequently lack common planktonic taxa, significantly hindering biostratigraphic analysis. Although it is possible to date correlative deep-water strata, this requires continuous outcrops (with limited or no soil or vegetation cover) and minimal tectonic disturbance, conditions that are rarely met in the Mediterranean region. Mediterranean Upper Miocene carbonates also lack other reliable biostratigraphic markers, such as high-diversity larger benthic foraminiferal assemblages (Cahuzac and Poignant, 1997). Furthermore, strontium isotope stratigraphy is hampered by the restricted circulation of the basin during the Late Miocene (Cornacchia et al., 2017).

To address this issue, the Upper Miocene was divided into two reasonably homogeneous intervals into which most of the successions could be confidently placed: the lower Tortonian and the upper Tortonian to pre-evaporitic Messinian. During the early Tortonian, the Mediterranean region was characterised by periods of increased precipitation (i.e., washhouse events; Böhme et al., 2011; Prista et al., 2015). The latest of these events occurred at approximately 8.9 Ma, marking a shift towards drier conditions that persisted for the remainder of the Miocene (Böhme et al., 2011; Prista et al., 2015). The early Tortonian was also characterised by higher temperatures (i.e., the Tortonian Thermal Maximum) than the late Tortonian and Messinian (Westerhold et al., 2020), with significant cooling recorded at around 8 Ma in the Mediterranean region (Tzanova et al., 2015). These environmental shifts are documented in shallow-water carbonates. Carbonate systems spanning the transition from the humid lower Tortonian to the more arid upper Tortonian record a shift from coralline algal-rich systems to coral-rich systems (e.g., the transition from the Lower Bar Unit to the Reefal Unit in Menorca; Obrador et al., 1992; Mateu-Vicens et al., 2008; Pomar et al., 2012; Brandano et al., 2016). At the Mediterranean scale, this boundary is associated with the expansion of coral-dominated shallow-water bioconstructions (Pomar and Hallock, 2007; Pomar et al., 2017; Cornacchia et al., 2021; Brandano et al., 2022). Consequently, the current study focuses on shallow-water carbonate systems which developed from the late Tortonian (i.e., after 9–8 Ma) to the early Messinian (before the onset of the Messinian Salinity Crisis) and that display relevant coral-dominated bioconstructions. Coeval carbonate systems dominated by heterozoan assemblages (e.g., Sola et al., 2022 and reference therein) were excluded, as they represent distinct environmental settings and comparing wildly different assemblages would result in their intrinsic ecological differences masking large-scale gradients. The investigated time-frame also offers a pragmatic compromise between stratigraphic accuracy and available data, as a "late Tortonian to early Messinian age" is often the only chronological information reported (e.g., Pedley and Grasso, 1994; Sola et al., 2017). Moreover, time intervals of similar or longer duration have been effectively utilized in recent reviews of the Upper Miocene fossil record (e.g., Agiadi et al., 2024a, 2024b).

2.2. Presence/Absence analysis

To compile the presence/absence database, published literature was reviewed for information on skeletal assemblages, considering only Upper Miocene carbonate systems characterised by coral-dominated, bioconstructions (reef-bearing systems) (Supplementary Table S1). The literature research began with the database of Esteban (1996) and the Paleo-Reef Database (Kiessling et al., 1999; Flügel and Kiessling, 2002), incorporating new findings from more recent papers. A total of 52 sites was considered (Fig. 1) (Supplementary Table S1). The presence/absence matrix consisted of the main groups of carbonate producers: colonial corals (CC), red calcareous algae (RCA), green calcareous algae (GCA, mainly represented by *Halimeda*), molluscs (MOL), echinoderms (ECH), benthic foraminifera (including large benthic foraminifera, LBF; small benthic foraminifera, SBF; encrusting benthic foraminifera, EBF), serpulids (SERP), bryozoans (BRY), ostracods (OSTR), and mobile arthropods (MA). A distinctive characteristic of ecological datasets consisting of presence/absence data is the tendency to have a large number of zero values (Clarke and Green, 1988); thus, they are strongly influenced by “true zeros” and “false zeros”. “True zeros” represent the absence of a certain category, whereas “false zeros” can result from sampling or observation errors. To avoid this issue (MacKenzie et al., 2002; MacKenzie, 2005), carbonate producers uncommon in Mediterranean's Upper Miocene shallow-water carbonates (e.g., barnacles, brachiopods, solitary corals and planktic foraminifera), were excluded from the presence/absence analysis, reducing the number of categories and of potentially “false zeros”. The frequency of the reported occurrence of the various carbonate producers in fossil sites (i.e., how frequent is the presence of a calcifier within the array of investigated sites) was compared with similar data calculated for a comprehensive database of modern allochem assemblages (Bialik et al., 2023, supplementary material), focusing at tropical (0–23°) and subtropical (23–40°) latitudes.

2.3. Quantitative microfacies analysis

For the quantitative microfacies analysis, five, upper Tortonian to lower Messinian fossil sites —Cyprus, Eratosthenes Seamount, Salento Peninsula, Acquabona, and Cariatiz (Fig. 1) —were selected based on existing information, focusing on photic-zone facies that either represent coral reefs or are directly related to them (e.g., fore-reef, lagoon). For the Eastern Mediterranean four localities from Cyprus and Site 966 from the Eratosthenes Seamount were considered, relying on the quantitative data provided in Coletti et al. (2019, 2020, 2021). From the Central Mediterranean, the site of Acquabona in northern Tuscany (Bossio et al., 1996) and three localities from the Salento Peninsula were investigated (Bosellini et al., 2001, 2002; Bosellini, 2006; Braga et al., 2009). Regarding the Acquabona site, the data provided in Coletti et al. (2024) were used. In the case of the Salento sites, the material previously studied by Bosellini et al. (2001, 2002) was reassessed through point-counting analysis of samples representative of the main facies. The Western Mediterranean material from the Cariatiz carbonate platform of the Sorbas Basin, previously investigated by Reolid et al. (2014, 2016, 2017a), was also reassessed with point-counting. In contrast to the presence/absence database, benthic foraminifera were categorized into LBF (large, symbiont-bearing), SBF (small, heterotrophic, free-living), and EBF (encrusting). While these groups were initially subdivided by test structure (hyaline, porcelaneous, agglutinated) during data acquisition, low occurrences in many samples necessitated grouping them for the ordination analysis (raw data remain available to allow for different analytical configurations).

Based on pre-existing knowledge of the sites, the samples were selected from the various facies of the investigated sites to capture the overall variability of the analysed systems. This resulted in 18, 55, and 53 thin sections for the Western, Central, and Eastern Mediterranean, respectively. In each section, more than 500 points were counted, resulting in a total of over 140,000 points (Supplementary Table S2). Six samples affected by diagenetic alteration were excluded from the following ordination analyses.

2.4. Ordination analysis

To account for the limitations of the datasets, both the presence/absence and the quantitative microfacies datasets were investigated using ordination analysis. Ordination analysis is widely used for data interpretation in the Earth Sciences, as it allows for studying a set of data while minimizing prior biases (Basso and Corselli, 2002; Bialik et al., 2021a). Similar objects are grouped closely together, and dissimilar objects are placed farther apart, highlighting complex relationships and exploring potential gradients among different sites (Gauch and Whittaker, 1972; Syms, 2008; Bialik et al., 2021a). These inherent properties of ordination analysis help addressing a potential limitation of this study: the representativeness of the investigated samples. Carbonate systems are vast, complex architectures whose total variability is notoriously difficult to assess (Pomar and Hallock, 2008; Brandano et al., 2022). While our sample selection was supported by extensive prior knowledge, the exploratory nature of the current research means that no established guidelines exist for determining a minimum number of samples necessary to achieve representativeness. However, since ordination techniques space samples according to their compositional similarity, the inclusion of “end-members” from the various facies ensures that the resulting multivariate space effectively brackets the system's full variability. In other words, by capturing the most divergent facies, the defined ordination area (i.e., the clusters of samples of the multivariate space) provides a proxy for the variability of the entire system, as any intermediate samples should mathematically fall within the established perimeter.

Two different types of ordination were used: Non-metric Multi-Dimensional Scaling (NMDS) and Detrended Correspondence Analysis (DCA). As an indirect gradient analysis, NMDS produces an ordination by replacing the original distance data with ranks, thereby avoiding issues associated with absolute distance (Kruskal, 1964). In contrast, DCA is a derivative of the correspondence analysis method (Hill, 1979). This methodology determines the relative position of elements by maximizing correspondence rather than variance between variables and data points. However, it suffers from creating often strong arch artefacts, a problem which is adjusted in the DCA, resulting in a better portrayal of the relationships between variables. Both NMDS and DCA analyses were performed using an updated version of the code for R software published by Bialik et al. (2021a) (the deployed code is provided in Supplementary Material 3). The Jaccard index (Jost et al., 2011) was used in the NMDS analysis of the presence/absence database. In contrast, the Bray-Curtis index (Bray and Curtis, 1957) was used for the quantitative microfacies dataset. In the latter case, to avoid issues related to uneven sample sizes and achieve a normal distribution of occurrence data, the Hellinger transformation (i.e., the square root of the relative abundances) was applied (Legendre and Gallagher, 2001; Legendre and Borcard, 2018).

The significance of the separation between the analysed populations (e.g., Eastern, Western, and Central Mediterranean sites) was evaluated using multivariate (MANOVA) and permutational (PERMANOVA) multivariate analyses of variance (Anderson, 2014). To verify the robustness of the ordination based on the quantitative microfacies dataset, multiple configurations were tried, using both NMDS and DCA. Initially, the entire dataset was tested. Subsequently, a sub-dataset comprising only colonial coral-rich facies was analysed. Finally, the coral-rich facies sub-dataset was tested, excluding corals from the ordination analysis. This step accounts for the potential sampling bias introduced by the limited spatial extent of thin sections, which may not adequately capture the heterogeneity of reef structures. For example, a sample from intra-reef sediments may contain few or no corals, whereas a sample from the reef framework may be entirely constituted by colonial corals, neither of which fully represents the compositional variability of the entire reef facies. Although the analysed samples were chosen to be as representative as possible of the large-scale variability of the facies investigated in the field, a “without-corals” analysis was also undertaken on the coral-rich facies sub-dataset to mitigate the potential bias related to the representativeness of thin sections from a reef. Moreover, given that the Eratosthenes reefal carbonates occur near the boundary between the humid and dry phases of the Tortonian (see the following section), the aforementioned analyses were performed both with and without the data from this site.

3. Geological setting of the basin and the studied sites

During the Miocene, the Mediterranean turned from a seaway connecting the Indo-Pacific and Atlantic Ocean into an enclosed basin (Dercourt et al., 2000). The eastern deep-water connection with the Indo-Pacific was severed during the Early Miocene, with most of the reduction occurring close to the Aquitanian-Burdigalian boundary, while a shallow seaway survived until the Serravallian (Aktaş and Robertson, 1984; Buchbinder, 1996; Rögl, 1999; Dercourt et al., 2000; Bialik et al., 2019, 2022). During the Late Miocene tectonic uplift of the Betic-Riffean orogenic arc at the westernmost end of the Mediterranean, resulted in the progressive restriction and subsequent sealing of the western straits, triggering the MSC (Hsü et al., 1973; Dercourt et al., 2000; Meilijson et al., 2019; Agiadi et al., 2024a, 2024b; Roveri et al., 2025). As the basin became increasingly isolated from the world's oceans, regional and global climates began a gradual cooling trend, particularly from the late Tortonian onward (Prista et al., 2015; Tzanova et al., 2015; Westerhold et al., 2020). Alongside this cooling, significant shifts in precipitation patterns occurred: prevailing humid conditions during the early-to-middle Tortonian gave way to more arid conditions throughout the remainder of the Miocene (Böhme et al., 2011). Notwithstanding restricted circulation and colder temperatures, during the Late Miocene, and particularly from the late Tortonian onward, shallow-water, coral-rich carbonate factories spread along the coasts of the Eastern, Central, and Western Mediterranean (Esteban, 1979, 1996; Pomar and Hallock, 2007; Perrin and Bosellini, 2012; Pomar et al., 2017) (Figs. 1, 2). These carbonate factories, usually featuring coral-rich facies and well-developed reefs, were significantly different from those of the Lower and Middle Miocene (e.g. Tomassetti et al., 2013; Vescogni et al., 2014; Coletti et al., 2021), chiefly by displaying a much lower coral biodiversity, often limited to only two genera, *Porites* and *Tarbellastraea* (Bosellini and Perrin, 2008; Perrin and Bosellini, 2012, 2013). This applies to all the Upper Miocene reef-bearing systems selected for the current analysis, which are synthetically detailed in the following paragraphs (Fig. 2).

The Upper Miocene carbonates of Cyprus and the Eratosthenes Seamount of the Eastern Mediterranean (Fig. 2A-D) developed during a relative sea-level fall connected to the complex convergence of African and Eurasian plates that involved the various terrains constituting the island of Cyprus and the Eratosthenes Continental Block (Mart and Robertson, 1998; Kinnaird and Robertson, 2013; Coletti et al., 2019, 2021; Cannings et al., 2021) (Fig. 2B, C). This tectonic process provided the substrate for these complex carbonate systems. The Upper Miocene shallow-water facies of the Eratosthenes Seamount (Fig. 2A) developed from the late Tortonian onward (around and after 8.4 Ma), and include a coral reef and a lagoon facies, the latter rich in molluscs and benthic foraminifera (Coletti et al., 2019; Coletti and Basso, 2020). Both facies were inferred to represent oligotrophic, warm-water settings (Coletti et al., 2019). The strata characterised by these facies are capped by a thin, ostracod-rich, limestone layer most likely related to a brackish environment developed during the initial phases of the MSC (Coletti et al., 2019).

In Cyprus, the shallow-water carbonates of the Koronia Member (Pakhna Formation) mainly deposited after 9.3 Ma in eastern Cyprus (Cannings et al., 2021) and after 7.7 Ma in western Cyprus (i.e., the source of most of the samples analysed in the present research) (Cannings et al., 2025) (Fig. 2D). Koronia Member carbonates outcrop along the northern margin of the Troodos Massif, on the flanks of Polis Graben, and in SE Cyprus (Fig. 2D), including both in situ coral-reefs and related facies and debris-talus derived from the fragmentation of the reefs (Follows and Robertson, 1990; Follows, 1992; Follows et al., 1996; Cannings et al., 2021; Coletti et al., 2021). Carbonates of the Koronia Member also occur around the southern margins of the Troodos Massif where they are mainly represented by redeposited materials, including large blocks and debris-flow deposits interbedded with deep-water facies (Robertson, 1977; Eaton and Robertson, 1993; Coletti et al., 2021) (Fig. 2D).

The Salento Peninsula is the southern portion of the Apulia Carbonate Platform, a thick carbonate sequence developed over a promontory of the African Plate (Fig. 2A, E), which collided with the Eurasian Plate following the closure of the Alpine Tethys (Bosellini et al., 1999; Rusciadelli et al., 2003; Muttoni et al., 2013). This southern Central Mediterranean succession includes an Upper Miocene portion, the Messinian Novaglie Formation (Bosellini et al., 1999) (Fig. 2E). The latter is divided into three superimposed depositional sequences (Bosellini et al., 2001). The lowermost and oldest unit (early Messinian, NF1) directly overlies the Oligocene and Cretaceous carbonate platforms (Bosellini et al., 2001). It is generally thicker in comparison to the overlying units (Bosellini et al., 2001; Vescogni et al., 2022) and exhibits a remarkable facies variability, including slope facies with *Halimeda* fragments and bioherms, as well as reef margin and back-reef facies (Bosellini et al., 2001). Due to this large variability, it was selected for the current research. It most likely developed in relatively warm, clear water, with no notable terrigenous input (Bosellini et al., 2001). The overlying sequence (NF2) is thinner and includes vermetid bioconstructions and coral reefs (Bosellini et al., 2001). It likely developed in conditions similar to those of NF1, although the presence of common vermetid bioconstructions might suggest slightly lower temperatures and, possibly, a higher nutrients supply (Bosellini et al., 2001). The younger, uppermost sequence (NF3) is characterised by a remarkable amount of microbial carbonates, which occur associated with both *Porites* and vermetid bioconstructions (Bosellini et al., 2001; Vescogni et al., 2022, 2025). This uppermost unit is considered a Terminal Carbonate Complex (sensu Esteban, 1979) and postdates the onset of the MSC (Vescogni et al., 2022, 2025; Vescogni and Guido, 2026).

The Messinian Calcare di Rosignano Formation developed along the eastern margin of the Tyrrhenian Basin (northern Central Mediterranean), within the Tora-Fine Basin (Bossio et al., 1993; Martini and Sagri, 1993) (Fig. 2A, F). It overlies Mesozoic igneous and sedimentary rocks (mostly Jurassic radiolarites, serpentinites, basalts, and gabbros, and Cretaceous deep-water sediments) remnants of the Ligure-Piemontese oceanic basin, and Tortonian to lower Messinian lacustrine sediments (Bossio et al., 1996) (Fig. 2F). The Calcare di Rosignano Formation includes basal conglomerates, large coral-dominated bioconstructions, and the related bioclastic carbonates, lagoonal bioclastic carbonates, and stromatolites (Fravega et al., 1994; Bossio et al., 1996). Based on its planktic foraminiferal assemblage, it has been attributed to the lower part of the Messinian (Bossio et al., 1996). The Acquabona Reef, analysed in this study, is an informal unit of the Calcare di Rosignano Formation and comprises the largest coral-dominated bioconstructions, along with coralline algal rudstone and serpulid floatstone to wackestone (Coletti et al., 2024). It developed in a warm climate under stressful conditions (i.e. restricted circulation and/or rapid fluctuations in temperature, nutrient availability and other environmental parameters), as indicated by the composition of the skeletal assemblage, which is dominated by corals at the base and by serpulids towards the top (Coletti et al., 2024).

The Sorbas Basin in southeastern Spain hosts several well-preserved carbonate platforms (Fig. 2A, G) (Martín and Braga, 1994; Reolid et al., 2017a). These include the Messinian Cariatiz Carbonate Platform, the margins of which display *Porites*-dominated coral-reefs (Fringing Reef Unit), serpulid-rich, *Halimeda*-rich, and siliciclastic-rich facies (Riding et al., 1991; Martín and Braga, 1994; Braga et al., 1996; Reolid et al., 2014, 2017a, 2017b) (Fig. 2G). This unit developed in a shallow coastal setting (with water depths of less than 50 m), characterised by substantial nutrient and siliciclastic inputs (possibly associated with

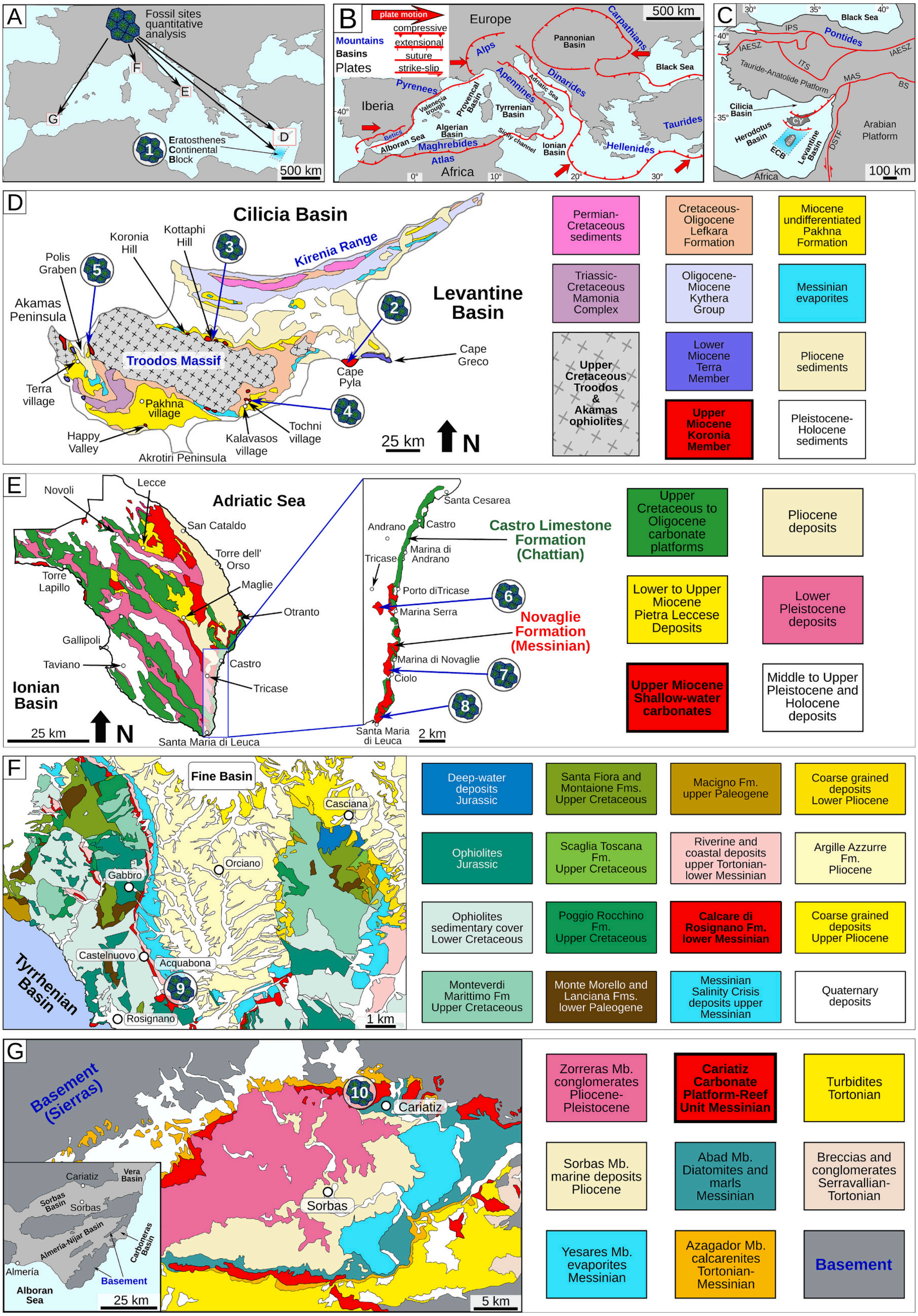

(caption on next page)

Fig. 2. Geological setting of the basin and of the studied sites. A) Current geography of the Mediterranean Basin indicating the position of the Upper Miocene sites investigated for the quantitative microfacies analysis and the location of the study-sites depicted in the panels; coordinates of the investigated fossil site from the Eratosthenes Seamount, 1 = 33.79°N, 32.70°E. B) Geological setting of the Mediterranean Basin with indicated the main tectonic lineaments, the main sub-basins and plate movements (adapted from Faccenna et al., 2004; Carminati and Doglioni, 2005; Carminati et al., 2012). C) Schematic tectonic map of the Eastern Mediterranean region showing the main tectonic features; BS = Bitlis Suture; DSTF = Dead Sea Transform Fault; ESM = Eratosthenes Seamount; ECB = Eratosthenes Continental Block; IAESZ = İzmir-Ankara-Erzincan Suture Zone; IPS = Intra-Pontide Suture; ITS = Inner Tauride suture; MAS = Misin-Andırın Suture (adapted from Robertson et al., 2013). D) Simplified geological map of Cyprus showing some of the main geological units; the shallow-water-carbonate of the Terra and Koronia members, comprising the Pakhna Formation, are indicated in bright blue and red respectively (adapted from Cannings et al., 2021); the investigated Upper Miocene fossil sites are indicated by the same symbol as in panel A and their coordinates are: 2 = 34.96 N°, 33.83°E, 3 = 35.05°N, 33.15°E; 4 = 34.78°N, 33.32°E; 5 = 34.98°N, 32,47°E. E) Simplified geological map of Salento peninsula showing some of its main geological units (adapted from Tancredi et al., 2022) with the Upper Miocene carbonates indicated in bright red; the focus on the Adriatic coast displays the main Cenozoic reef units (adapted from Bosellini, 2006) and the investigated Upper Miocene sites whose coordinates are: 6 = 39.91°N, 18.36°E; 7 = 39.84°N, 18.38°E; 8 = 39.80°N, 18.37°E. F) Simplified geological map of Fine Basin and the nearby areas showing the main geological units among which the Upper Miocene carbonates are indicated in bright red (adapted from Mazzanti et al., 2016); the coordinates of the studied site (9) are 43.41°N, 10.47°E. G) Simplified geological map of the Sorbas Basin indicating the main geological units and the basement of the basin and the Upper Miocene carbonates highlighted by the bright red colour (adapted from Nooitgedacht et al., 2018); the coordinates of the studied site (10) are 37.14°N, −2.09°E; the inset panel displays the overall geological setting of the Cenozoic basins of the area (adapted from Reolid et al., 2017a). (For interpretation of the references to colour in this figure legend, the reader is referred to the web version of this article.)

freshwater influxes), which fostered the development of both *Halimeda* and serpulid accumulations (Braga and Martin, 1996; Reolid et al., 2017a).

4. Results

4.1. Presence/absence of carbonate producers

The most frequent carbonate producers within the 52 described Upper Miocene, reef-bearing systems, are: colonial corals (CC), molluscs (MOL), red calcareous algae (RCA), benthic foraminifera (BF; including both small, large and encrusting taxa since the separation between them was often not indicated), echinoderms (ECH), and bryozoans (BRY). The first three groups are reported in over 90% of the sites (Supplementary Table S1). Benthic foraminifera are reported from over 80% of the sites. Bryozoans (BRY) and echinoderms (ECH) are reported in more than 2/3 of the sites, serpulids (SERP) in 1/2 of the sites, and green calcareous algae (GCA) in roughly 1/3 of the sites (Supplementary Table S1). When considering only the 40 sites spanning from the upper Tortonian to the pre-evaporitic Messinian, this pattern remains virtually unchanged; only a slight increase in the relative frequency of occurrence of bryozoans and echinoderms is observed (Supplementary Table S1).

In ordination analysis, the vectors relative to the various types of carbonate producers are arranged radially, and do not show a meaningful clustering (Fig. 3). Axis 1 is divided between colonial corals, red algae, and echinoderms on one side and ostracods, green algae, bryozoans, serpulids, and mobile arthropods on the other. Axis 2 is mainly expressed by the mobile arthropods and echinoderms in one direction, and less defined in the other. Molluscs and benthic foraminifera do not contribute much to the variance in either axis. Within NMDS space, the Western, Central and Eastern Mediterranean carbonates exhibit a large overlap towards the centre of the plot (Fig. 3A). Towards the periphery, the three clusters slightly extend outwards from the overlap zone in different directions, but the data populations from the sub-basins are statistically similar ($p >> 0.05$ in MANOVA test for all combinations) (Fig. 3). Grouping the sites by age within the same plot reveals no clear pattern, with the variability of lower Tortonian sites overlapping almost completely with later sites (Fig. 3B). Similarly, the NMDS analysis performed exclusively on upper Tortonian to pre-evaporitic Messinian sites shows no significant trend (Fig. 3C). The lack of an Eastern Mediterranean cluster is due to the presence of only two sites that can be confidently assigned to the upper Tortonian, which is insufficient to generate a cluster (Fig. 3C).

4.2. Quantitative analysis of the skeletal assemblages

Overall, among the investigated samples, the most prevalent producers are RCA (mainly encrusting taxa) and CC (Fig. 4A-D; Table 1). Encrusting benthic foraminifera (EBF, mainly represented by porcelaneous taxa of the Nubeculariidae family and, to a lesser extent, by

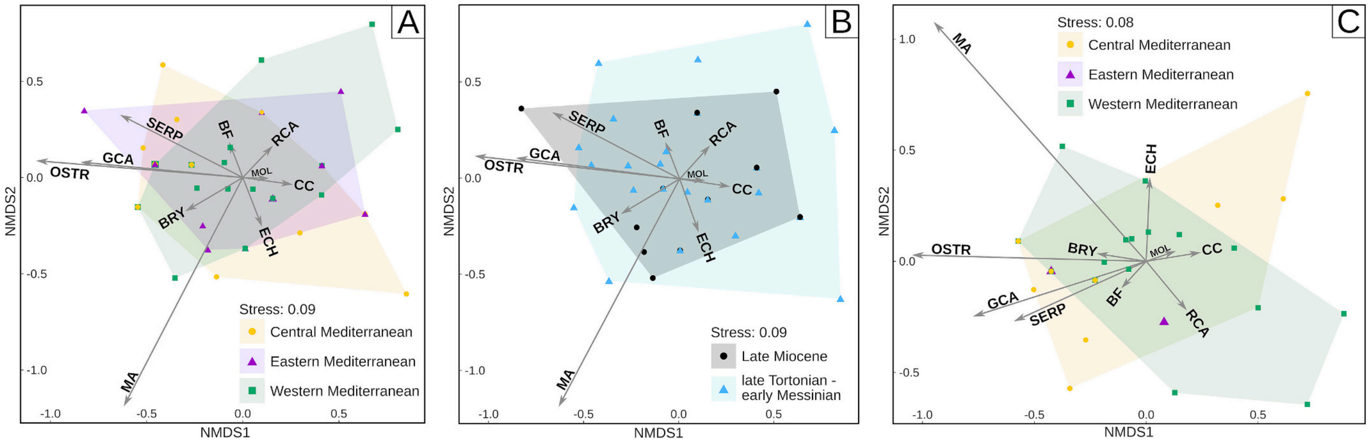

Fig. 3. NMDS analysis based on the presence absence database built upon literature data; RCA = red calcareous algae; CC = colonial corals; MOL = molluscs; BF = benthic foraminifera; SERP = serpulids; GCA = green calcareous algae; OSTR = ostracods; BRY = bryozoans; MA = mobile arthropods such as decapod crustaceans; ECH = echinoderms. A) All Upper Miocene systems clustered on basis of the sub-basin. B) All Upper Miocene systems clustered on the basis of the time interval. C) Only Upper Miocene systems deposited between the late Tortonian and the early Messinian (before the MSC); note that in this analysis a cluster of data points for the Eastern Mediterranean can't be generated as only two points are available. (For interpretation of the references to colour in this figure legend, the reader is referred to the web version of this article.)

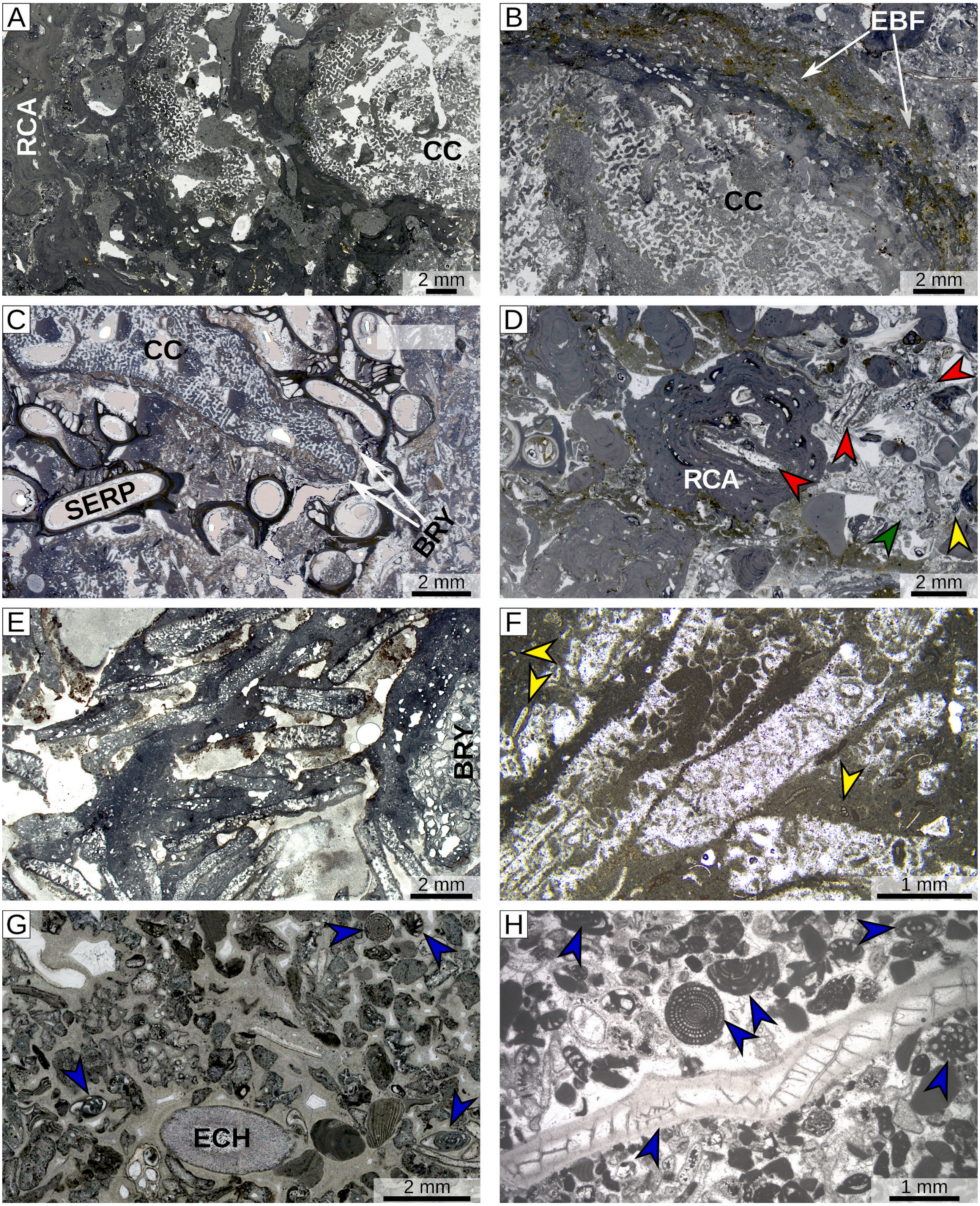

Fig. 4. Relevant microfacies of the analysed Upper Miocene, reef-bearing, carbonate systems. A) Eastern Mediterranean, Cyprus, Kottaphi Hill, coral boundstone; CC = colonial corals; RCA = red calcareous algae. B) Central Mediterranean, Acquabona, Fine Basin, coral boundstone; CC = colonial corals; EBF = encrusting benthic foraminifera. C) Western Mediterranean, Cariatiz Platform, Sorbas Basin, coral-rich facies; CC = colonial corals; SERP = serpulids; BRY = bryozoans. D) Central Mediterranean, Acquabona, Fine Basin, coral-bearing coralline algal rudstone; RCA = red calcareous algae; red arrowheads = *Halimeda*; green arrowhead = colonial coral fragment; yellow arrowhead = small benthic foraminifera. E) Western Mediterranean, Cariatiz Platform, Sorbas Basin, *Halimeda* facies; BRY = bryozoans. F) Central Mediterranean, Salento Peninsula, *Halimeda* facies; yellow arrowheads = small benthic foraminifera. G) Eastern Mediterranean, Eratosthenes Seamount, coral-rich lagoonal facies; blue arrowheads = symbiont bearing large benthic foraminifera; ECH = echinoderms. H) Eastern Mediterranean, Cyprus, Tochni village, coral-bearing lagoonal facies; blue arrowheads = symbiont bearing large benthic foraminifera, the large specimen at the centre of the field belongs to the genus *Heterostegina.* (For interpretation of the references to colour in this figure legend, the reader is referred to the web version of this article.)

Table 1
Average relative skeletal assemblage composition for the investigated Upper Miocene reef-bearing carbonate systems expressed as percentages; detailed data of skeletal assemblages composition are included in Supplementary Table S2.

All examined facies.	Eratosthenes	Cyprus	Salento	Acquabona	Cariatiz
Colonial corals (CC)	20	19	25	27	20
Red Calcareous Algae (RCA)	32	42	25	30	24
Green Calcareous Algae (GCA)	>1	1	8	2	6
Large Benthic Foraminifera (LBF)	9	4	<1	<1	<1
Encrusting Benthic Foraminifera (EBF)	8	19	10	5	<1
Small Benthic Foraminifera (SBF)	15	4	9	4	1
Molluscs (MOL)	10	3	8	5	8
Bryozoans (BRY)	1	1	5	2	15
Echinoderms (ECH)	3	3	3	7	3
Serpulids (SERP)	<1	1	3	9	20
Ostracods (OSTR)	<1	<1	1	<1	<1
Mobile Arthropods (MA)	1	2	2	8	<1
Only coral-rich facies					
Colonial corals (CC)	20	24	37	30	24
Red Calcareous Algae (RCA)	32	35	22	35	28
Green Calcareous Algae (GCA)	<1	<1	3	3	2
Large Benthic Foraminifera (LBF)	9	3	<1	<1	<1
Encrusting Benthic Foraminifera (EBF)	8	24	13	6	<1
Small Benthic Foraminifera (SBF)	15	2	5	3	2
Molluscs (MOL)	10	4	6	5	8
Bryozoans (BRY)	1	<1	7	2	13
Echinoderms (ECH)	3	3	2	5	4
Serpulids (SERP)	<1	1	2	1	17
Ostracods (OSTR)	<1	<1	<1	<1	<1
Mobile Arthropods (MA)	1	2	1	9	<1

hyaline taxa of the Homotrematidae family) are common and represent the third most relevant build-up-builders (among the examined samples), except for the Cariatiz Platform of the Sorbas Basin (Fig. 4B, C; Table 1).

GCA (mainly represented by *Halimeda*) and SERP (mainly encrusting taxa) occur in some samples and, locally, can dominate the skeletal assemblage (Fig. 4C-F). Small benthic foraminifera (SBF), MOL, BRY, and ECH occur as minor components in most samples and sometimes they can be relatively abundant (Fig. 4D-G), especially SBF (Table 1). Large benthic foraminifera (LBF) are generally rare (mainly represented by *Dendritina*, *Borelis*, and *Heterostegina*) (Fig. 4G, H). They are relevant only in certain samples from the Eastern Mediterranean, specifically those from Cyprus and the Eratosthenes Seamount (Fig. 4G, H), and are very rare in samples from the rest of the basin. Mobile arthropods (MA), such as crabs and shrimps, are generally rare, except at the Acquabona site, where they are common in some samples. Ostracods (OSTR) are generally very rare.

Two main vector clusters can be recognized across all plots (all the data, Fig. 5; only coral-rich facies, Fig. 6; only coral-rich facies excluding colonial corals as a variable, Fig. 7), and in particular in the NDMS plot of the complete dataset (Fig. 5A). These vector clusters represent most of the variability along the first axis of most plots (e.g., Figs. 5A, 6A, B, 7A). One cluster includes CC, RCA, and EBF, while another is typically oriented in the opposite direction and is more weakly defined (Figs. 5–7). This other cluster typically includes GCA, MOL, ECH, and LBF but SBF, OSTR, and, more rarely, SERP may also be present. The first cluster of vectors mainly correspond to the main build-up-builders, while the second cluster primarily consists of bioclast-producers (Figs. 5–7). MOL, ECH, and RCA vectors are usually small, as these carbonate producers show limited variability among the analysed samples. Except for the DCA analysis based only on coral-rich facies and excluding corals as a variable (Fig. 7B, D), all plots show the proximity of SERP and BRY vectors, highlighting the strong relationship between bryozoan and serpulid distributions (Figs. 5–7). These two vectors are also typically representative of a significant portion of the variability along the vertical axis. The LBF and EBF vectors are always nearly opposite one another, indicating a widely different distribution for these groups of benthic foraminifera (Figs. 5–7).

In most analyses, it is evident that the areas including samples from the two Eastern Mediterranean sites exhibit a remarkable degree of overlap (Figs. 5A, B, 6B, 7B). The field including samples from the Salento peninsula, located in the southern Central Mediterranean, overlaps with both Eastern Mediterranean sites (Figs. 5–7). The area of Acquabona, located in the northern Central Mediterranean, is instead more often stretched towards the SERP vector (Figs. 5A, B, 7A). The Western Mediterranean site of Sorbas shows a lower overlap with the other sites, particularly with the Eastern Mediterranean sites, and it is significantly more stretched towards the SERP and BRY vectors (Figs. 5–7). This pattern is particularly evident in both DCA analyses based on datasets with only coral-rich facies (Figs. 6B and 7B).

Overall, all the plots (Figs. 5–7) show a comparable distribution, despite differences in both the underlying datasets and in the analysed variables. The plots based only on coral-rich facies, show a smaller scatter of the samples (as expected), particularly those generated using the NMDS methodology (Figs. 6A, 7A). The removal of corals as a variable appears to not significantly alter the overall outline of the plot, nor the relative position and direction of the vectors. Indeed, the cluster of vectors related to build-up-builders (in this case, mainly represented by RCA and EBF) remains clearly visible and displays the same orientation relative to the cluster of vectors representing bioclast-producers. All the above-mentioned patterns remain unchanged if the Eratosthenes Seamount (ESM in the plots) is removed from the analysis, which is consistent with its significant overlap with the nearby Cyprus site (i.e. the overall variability of the Eratosthenes Seamount is largely comprised in the variability of Cyprus and thus its removal does not affect the structure of the plot) (Figs. 5C, D, 6C, D, 7C, D).

Statistically, the sites are separated. The MANOVA test shows that all sites were significantly different ($p < 0.05$), except for Salento and Eratosthenes ($p = 0.06$). The PERMANOVA test, more representative of the NMDS space, only showed Cyprus as being distinct from all other sites ($p << 0.05$), although its differentiation from the Eratosthenes was marginal ($p = 0.049$) (Supplementary Table S2). Sorbas was distinct

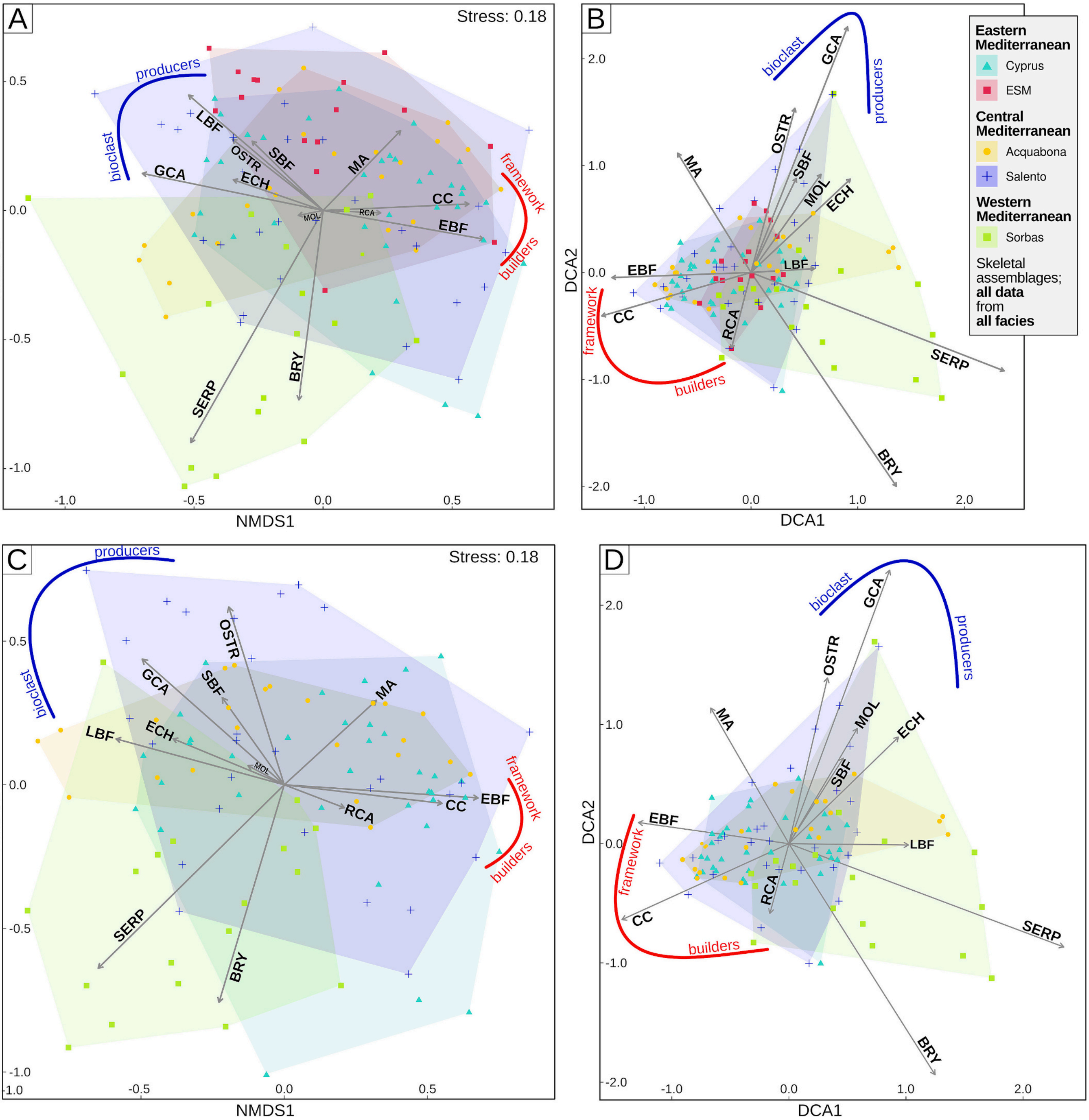

Fig. 5. NMDS and DCA plots based on the database resulting from the quantitative microfacies analysis of the Upper Miocene sites; the depicted plots are based on the run including all reef and reef-related facies; bioclast acronyms are as in indicated in the text and in the caption of Fig. 3. A) NMDS based on the data from the Eratosthenes Seamount (ESM), Cyprus, Salento, Acquabona and Sorbas sites. B) DCA based on the data from the Eratosthenes Seamount (ESM), Cyprus, Salento, Acquabona and Sorbas sites. C) NMDS analysis excluding samples from the Eratosthenes Seamount. D) DCA analysis excluding samples from the Eratosthenes Seamount.

from all sites except Acquabona ($p = 0.07$) and close but distinct from Salento ($p = 0.03$). The Eratosthenes, Salento, and Acquabona were not found to be distinct ($p > 0.05$) (Supplementary Table S2).

5. Discussion

5.1. Presence/absence analysis

Many of the 52 Upper Miocene carbonate systems included in the analysis have been described in a single paper. In cases where the site was revisited, differences in methodology and scientific focus often resulted in differences in what was reported. For these reasons, the presence/absence dataset provides only a broad overview of these carbonate factories. The ordination analysis reflects this. The groups of samples from the Western, Central, and Eastern Mediterranean display a considerable overlap and display no statistically significant differences among them (Fig. 3). The distribution of the vectors does not display any discernible environmental gradient or pattern associated with the

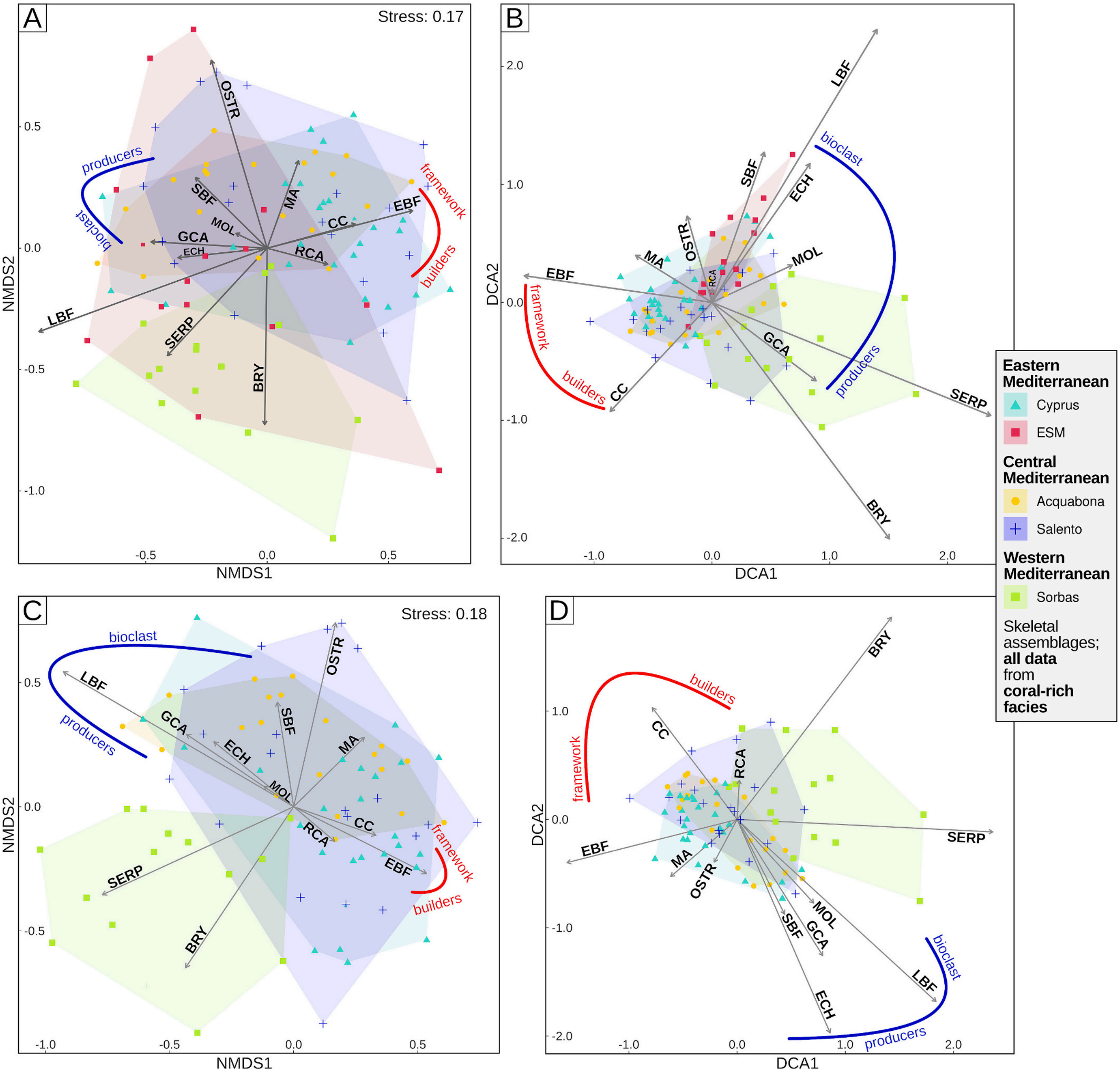

Fig. 6. NMDS and DCA plots based on the database resulting from the quantitative microfacies analysis; the depicted plots are based on the run including only data from coral-rich facies; bioclast acronyms are as in indicated in the text and in the caption of Fig. 3. A) NMDS based on the data from the Eratosthenes Seamount (ESM), Cyprus, Salento, Acquabona and Sorbas sites. B) DCA based on the data from the Eratosthenes Seamount (ESM), Cyprus, Salento, Acquabona and Sorbas sites. C) NMDS analysis excluding samples from the Eratosthenes Seamount. D) DCA analysis excluding samples from the Eratosthenes Seamount.

distribution of carbonate producers, neither in the analysis with all Upper Miocene systems nor in that focusing solely on sites of unambiguous post-early Tortonian age (Fig. 3). The presence/absence analysis is also unable to resolve the shift in carbonate factory composition from the lower to the upper Tortonian (Fig. 3).

Despite the aforementioned limitations, when comparing fossil and modern assemblages in terms of frequency of occurrence (i.e., the frequency with which certain types of carbonate producers are present in the various sites considered in the analysis) a significant difference in the frequency of green calcareous algae emerges. In modern, shallow-water, tropical carbonate factories, colonial corals, benthic foraminifera, molluscs, and red calcareous algae are the dominant organisms in the vast majority of cases (Bialik et al., 2023, supplementary materials). These carbonate producers are reported, in various amounts, from over 90% of modern sites located at tropical (0–23°) and subtropical latitudes (23–40°), with the only exception of colonial corals, which occur in 2/3 of sites at subtropical latitudes compared to >90% of tropical latitudes (Bialik et al., 2023, supplementary material). Green calcareous algae (mainly represented by the genus *Halimeda*) also occur in the majority of modern tropical sites (~80%) and in half of subtropical ones (Bialik et al., 2023, supplementary material). Whereas colonial corals, benthic foraminifera, and red calcareous algae occur in the vast majority of examined Upper Miocene sites (> 90%), green calcareous algae (mainly *Halimeda*) are reported from only about 1/3 of them. This suggests that Mediterranean Upper Miocene carbonate factories were more similar to modern subtropical factories than to tropical ones. In

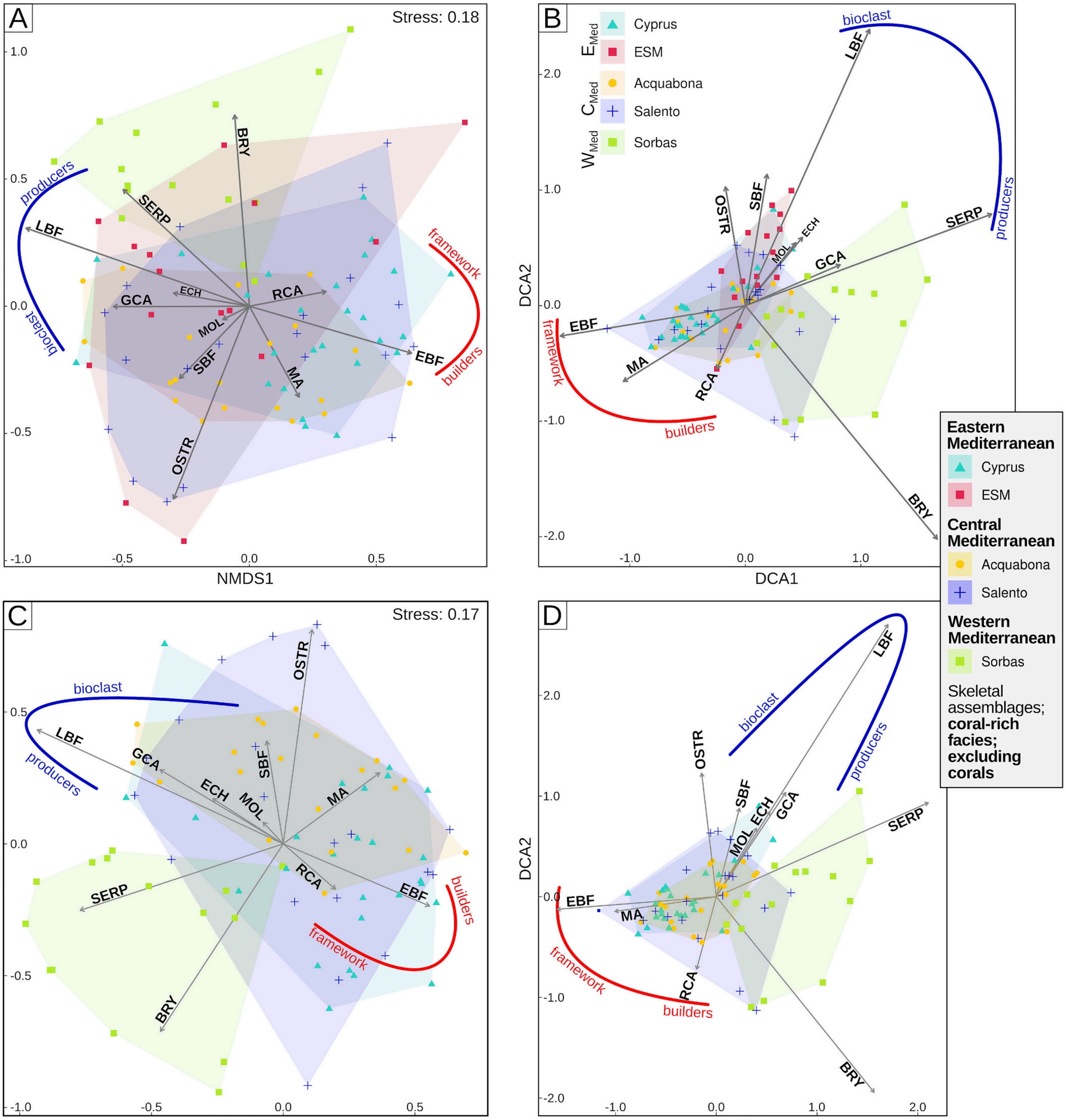

Fig. 7. NMDS and DCA plots based on the database resulting from the quantitative microfacies analysis; the depicted plots are based on the run including only data from coral-rich facies and excludes colonial corals from the variable; bioclast acronyms are as in indicated in the text and in the caption of Fig. 3. A) NMDS based on the data from the Eratosthenes Seamount (ESM), Cyprus, Salento, Acquabona and Sorbas sites. B) DCA based on the data from the Eratosthenes Seamount (ESM), Cyprus, Salento, Acquabona and Sorbas sites. C) NMDS analysis excluding samples from the Eratosthenes Seamount. D) DCA analysis excluding samples from the Eratosthenes Seamount.

modern studies, *Halimeda* is indeed more thermally sensitive than red calcareous algae (but less sensitive than reef corals) (Anton et al., 2020; Khen et al., 2025), and it has a thermal optimum higher than that of common red calcareous algae (Anton et al., 2020). Moreover, heavily calcified lineages are usually more abundant in tropical conditions (Verbruggen and Kooistra, 2004). It is also worth noting that Neogene green calcareous algal skeletons are constituted of loosely bounded aragonite crystals (Granier, 2012); therefore, they have a much lower preservation potential than either molluscs, red calcareous algae, or colonial corals, whose skeletons are either more robust (e.g., corals) and/or more chemically stable (e.g., red calcareous algae). Therefore, whilst well-preserved *Halimeda* accumulations exists in specific investigated sites (e.g., Salento, Passaseo and Morsilli, 2025), a degree of preservation bias at the basin scale cannot be entirely dismissed. Overall, the scarcity of green calcareous algae in these Upper Miocene shallow-water systems, compared to modern counterparts, might reflect the relatively cool subtropical climate of the region, which was likely suboptimal for heavily calcified species of *Halimeda*. Although this scarcity may have been further compounded by a preservation bias linked to the inherent fragility and mineralogy of green calcareous algae skeletal remains, the overall trend underscores the existing positive correlation between temperature and the relevance of *Halimeda*-derived carbonate production (Bialik et al., 2023). Indeed, as Mediterranean temperatures rise due to global warming, heavily calcified species with a high carbonate production potential are already colonizing the basin (e.g., *Halimeda incrassata* Lamouroux, 1816) (Alós et al., 2016).

Upper Miocene shallow-water carbonate systems also exhibit a limited biodiversity of colonial corals and large benthic foraminifera (Cahuzac and Poignant, 1997; Bosellini and Perrin, 2008; Perrin and Bosellini, 2013; Agiadi et al., 2024a, 2024b). Uncommon GCA, and low symbiont-bearing colonial coral and LBF biodiversity are all consistent with subtropical conditions and in agreement with palaeoclimatic (Prista et al., 2015), palaeoecological (Bosellini and Perrin, 2008), and palaeogeographic reconstructions (Dercourt et al., 2000; Vaes et al., 2023).

5.2. Quantitative analysis of the skeletal assemblages

The quantitative microfacies study highlights an overall scarcity of LBF (Table 1), a group of carbonate producers that, as a whole, is generally favoured by warm periods (Coletti et al., 2022). Their scarcity is consistent with subtropical conditions indicated by palaeogeographic reconstructions (Dercourt et al., 2000; Vaes et al., 2023), low occurrence of *Halimeda*, and low biodiversity of colonial corals and of LBF themselves (Veron and Minchin, 1992; Cahuzac and Poignant, 1997; Chen, 1999; Beavington-Penney and Racey, 2004; Bosellini and Perrin, 2008; Perrin and Bosellini, 2013). The quantitative analysis is not only suggestive of subtropical conditions, it also suggests the presence of a basin-wide temperature gradient. LBF are more relevant in fossil sites from the Eastern Mediterranean (where they can locally dominate the assemblage) and rare elsewhere (Table 1; Supplementary Table S2). Existing data on the uppermost Miocene shallow-water carbonates of the southern Central Mediterranean also indicate that the contribution of LBF in this region might have been relevant. LBF-dominated facies are indeed reported by Di Credico et al. (2004) in Lampedusa and by Bialik et al. (2021b) in Malta. In the latter case, LBF dominated-facies occur at the top of the succession, strongly supporting a Messinian age (Bialik et al., 2021b). Based on the relationship between LBF abundance and temperature, this overall pattern is suggestive of a late Tortonian to early Messinian temperature gradient between a warm Eastern and a cooler Western Mediterranean, much like it is today (Pastor et al., 2019).

EBF and in particular nubeculariids are more common in eastern and southern sites than in northern and western ones (Table 1). Modern *Nubecularia* has been associated with shallow and lagoonal settings (Wisshak and Rüggeberg, 2006; Tichenor and Lewis, 2018) and the common species *Nubecularia lucifuga* (Defrance, 1825) is frequently found in seagrass meadows (Mateu-Vicens et al., 2014). On the other hand, Miocene *Nubecularia* has been related to shallow, restricted and stressful environments (Piller and Harzhauser, 2024). *Nubecularia* reefs are a common feature of the Sarmatian of the Paratethys, dating to when the basin became semi-enclosed, causing environmental conditions to deviate significantly from normal marine settings (Pisera, 1996). This affinity for restricted environments contrasts sharply with modern counterparts like *N. lucifuga*. Furthermore, as modern nubeculariids do not form thick, extensive crusts comparable to those in the fossil record, it is highly probable that the observed fossil forms represent distinct taxa adapted to shallow, warm, and stressful conditions.

Ordination analysis based on quantitative data produces a substantially more informative pattern than presence/absence analysis (Figs. 3, 5, 6, 7). The disposition of the vectors highlights the two main styles of carbonate production in the examined upper Tortonian to pre-evaporitic Messinian systems: framework production and bioclastic production (Figs. 5–7). The quantitatively most relevant builders of the examined systems, namely colonial corals, red calcareous algae, and EBF, belong to the first group. Serpulids and bryozoans are also capable of developing reefs (Smith, 1995; Fornós et al., 1997; Riedi and Smith, 2015; Bastos et al., 2018; Kočí et al., 2021; Montefalcone et al., 2022; Rosso et al., 2023), but they form their own distinct group of vectors, usually orthogonal to those of all other framework-builders. This is likely due to their different environmental preferences. The abundance of colonial corals and red calcareous algae is positively correlated with light availability (Bialik et al., 2023). Nubeculariidae and Homotrematidae (the most common groups of EBF in the examined samples), prefer shallow-water environments in modern reefs (Walker et al., 2011; Tichenor and Lewis, 2018). On the other hand, the abundance of bryozoans and serpulids is negatively correlated with light availability (Bialik et al., 2023). Moreover, serpulids, unlike most of reef-corals, frequently develop bioconstructions in areas of reduced water turbulence (Bosence, 1973; Fornós et al., 1997; Rovere et al., 2015). Consequently, the abundance of these two sets of framework builders is unlikely to be correlated, explaining why their respective vector clusters point in different directions.

The bundle of vectors related to bioclast-producers includes green calcareous algae, SBF, LBF, echinoderms, molluscs, and ostracods. These calcifiers do not share the same trophic habit (i.e., some are heterotrophs, others are autotrophs, and others are mixotrophs). They are likely grouped because they primarily occur in settings other than the reef (e.g., lagoons). When ordination analysis is performed on a similar but larger dataset, encompassing skeletal assemblages from euphotic to oligophotic settings from all latitudes, carbonate producers end up grouped based on their trophic habit (i.e., all mixotrophs and autotrophs together) (Mutti and Hallock, 2003; Bialik et al., 2023). However, in our case study (i.e., the Upper Miocene of the Mediterranean), the overall variability of the skeletal assemblage dataset is significantly lower than in the aforementioned global analyses, allowing for a clear distinction between build-up-builders (reef) and bioclast-producers (e.g., lagoon) to emerge. The only carbonate producers whose position is not entirely fitting with this explanation are green calcareous algae. *Halimeda* is indeed a major producer of bioclasts (Bialik et al., 2023), but can also develop bioherms (Marshall and Davies, 1988; Braga et al., 1996; Martín et al., 1997; McNeil et al., 2016, 2021, 2022; Reolid et al., 2024). However, since these build-ups lack the sturdiness of coral reefs, it is easy to understand why green calcareous algae cluster together with the other bioclast-producers.

The ordination plots also highlight relevant patterns concerning encrusting and large benthic foraminifera. EBF and LBF are both relevant producers in the geological record of shallow-marine settings (Plaziat and Perrin, 1992; Coletti et al., 2022; Granier, 2024). Very commonly, in microfacies analysis, these two groups are reported together, despite their distinctly different ecological strategies, which clearly emerge in the current analysis where their relative vectors are always oriented in opposite directions. This indicates that they should always be reported separately.

Unlike the ordination analysis based on presence/absence data (Fig. 3), the ordination analyses based on quantitative data reveal that the areas of the samples from the Eastern, Central, and in particular the Western Mediterranean, do not entirely overlap (Figs. 5–7). This indicates that the overall variability of the examined systems, reflected by their spread across the ordination plot, displays distinct differences (e.g., the maximum abundance of a given carbonate producer frequently exceeds its abundance at other sites). This clear separation is consistent with the results of statistical analyses (i.e. MANOVA and PERMANOVA) and with the underlying environmental conditions of the investigated sites.

Indeed, Cyprus, Eratosthenes Seamount, and Salento developed in oligotrophic settings away from significant sources of terrigenous fluxes (Bosellini et al., 2001; Coletti et al., 2019, 2021). On the other hand, the Cariatiz Carbonate Platform of the Sorbas Basin was located close to emerging landmasses and was characterised by more relevant terrigenous fluxes (Reolid et al., 2014, 2017a). These detrital fluxes from the continent may have provided nutrients to the carbonate factory while reducing light penetration at the bottom, favouring heterotrophs (in particular serpulids) over phototrophs and mixotrophs (Reolid et al., 2017a). Serpulids might have been favoured also by fresh water influx from the mainland (Reolid et al., 2017a). However, another relevant element needs to be addressed here: the Sorbas Basin was in the Western Mediterranan, much closer and better connected to the cooler and more nutrient-rich Atlantic Ocean. Consistent with the effect of a basin-scale palaeoenvironmental gradient, the clusters of the Central Mediterranean sites frequently extend midway between the Western and the Eastern Mediterranean clusters, particularly in the DCA analyses (Figs. 5A, B, 6B, 7B). In agreement with statistical analyses, the Sorbas site also displays a wider overlap with Central Mediterranean sites than with Eastern Mediterranean ones (Figs. 5–7). Furthermore, by excluding the Sorbas site and running an additional ordination analysis focused solely on coral-rich facies (thereby reducing overall dataset variability to better reveal existing trends while compensating for the fewer data points), the East–West palaeoenvironmental gradient delineated by serpulids, bryozoans, and LBF remains visible, albeit less pronounced (Fig. 8). The Eastern Mediterranean remains the basin sector most extended along the LBF axis (i.e., warmer temperatures), whereas the Central Mediterranean extends more along both the SERP and BRY axes

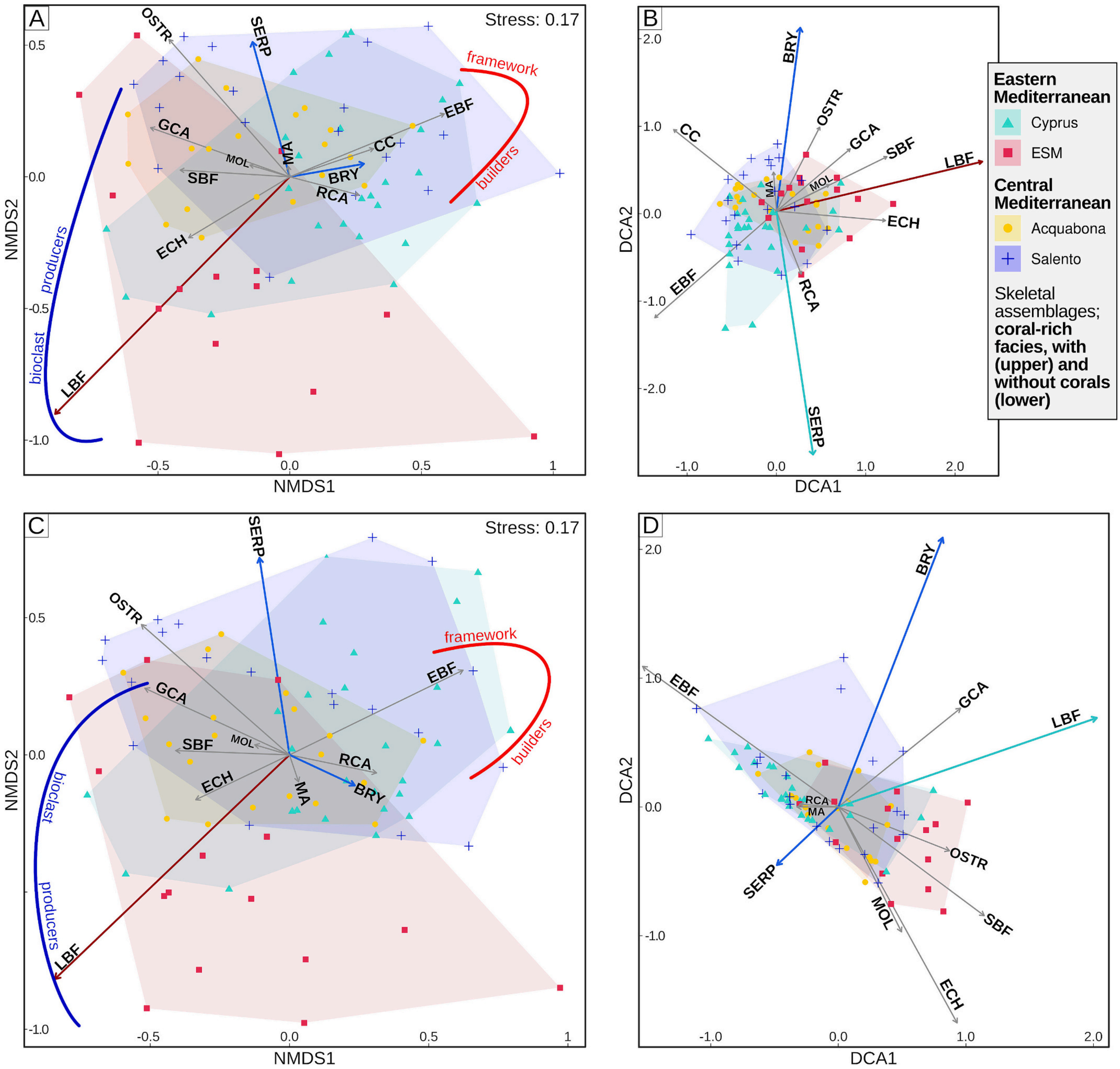

Fig. 8. NMDS and DCA plots based on the database resulting from the quantitative microfacies analysis of coral-rich facies, excluding data from the Sorbas Basin; bioclast acronyms are as in indicated in the text and in the caption of Fig. 3; the LBF, SERP and BRY vectors are highlighted in different colours, reflecting the site more stretched along the axis. A) NMDS plot with data from coral-rich facies and based on the run including colonial corals as a variable. B) DCA plot with data from coral-rich facies and based on the run including colonial corals as a variable. C) NMDS plot with data from coral-rich facies and based on the run excluding colonial corals as a variable. D) DCA plot with data from coral-rich facies and based on the run excluding colonial corals as a variable.

(more nutrients and/or lower temperatures) (Fig. 8). This underscores the consistency between an East–West palaeoenvironmental gradient and the overall variability of the analysed systems, as captured by the quantitative microfacies analysis and framed within the ordination space. Thus, while the position of Sorbas might be driven also by local factors, the overall distribution of samples remains consistent with a basin-scale paleoenvironmental gradient.

This palaeoenvironmental gradient aligns with the distribution of shallow-water, heterozoan-dominated facies from the upper Tortonian to the pre-evaporitic Messinian interval. Indeed, these facies are frequent in Western Mediterranean successions (e.g., Brachert et al., 1998; Martín et al., 2012; Sola et al., 2017, 2022, and references therein). In the Central Mediterranean, heterozoan shallow-water carbonates are rare; furthermore, while the Western Mediterranean heterozoan units are usually devoid of colonial corals (e.g., Sola et al., 2017), some Central Mediterranean equivalents include coral-dominated bioconstructions (e.g., Gramigna et al., 2012; Caracciolo et al., 2013). Finally, in the Eastern Mediterranean uppermost Miocene record, these heterozoan facies are essentially absent, and shallow-water carbonates are dominated by the photozoan assemblage (Follows, 1992; Eaton and Robertson, 1993; Coletti et al., 2019, 2021).

This overall pattern, from an oligotrophic and warmer Eastern Mediterranean to a more nutrient-rich and cooler Western Mediterranean, mirrors the present-day Mediterranean (Fig. 9). The western basin, which is closer to the connection with the Atlantic Ocean, displays cooler water and a higher primary productivity than the eastern one, resulting in a gradient of decreasing primary productivity and increasing temperature from West to East (Antoine et al., 1995; Bosc et al., 2004) (Fig. 9). During most of the Late Miocene, the Mediterranean's water exchange with the global ocean occurred primarily with the Atlantic via its western gateway(s), similarly as it occurs today (Cornacchia et al., 2018; Bialik et al., 2019; Capella et al., 2019; Reolid et al., 2022). Thus, it is most likely that an environmental gradient similar to the one that exists today was also present during most of the Late Miocene (Fig. 9). This hypothesis does not negate the effect of local factors, nor does it downplay the relevance of small-scale palaeoceanographic and palaeoclimatic events, which certainly influenced shallow-water carbonate production across the Mediterranean, particularly during the investigated interval, when the connectivity between different water masses was progressively decreasing (Cornacchia et al., 2026). Instead, it merely suggests that, in line with the current analyses and available evidence, the individual sectors were oscillating around distinct

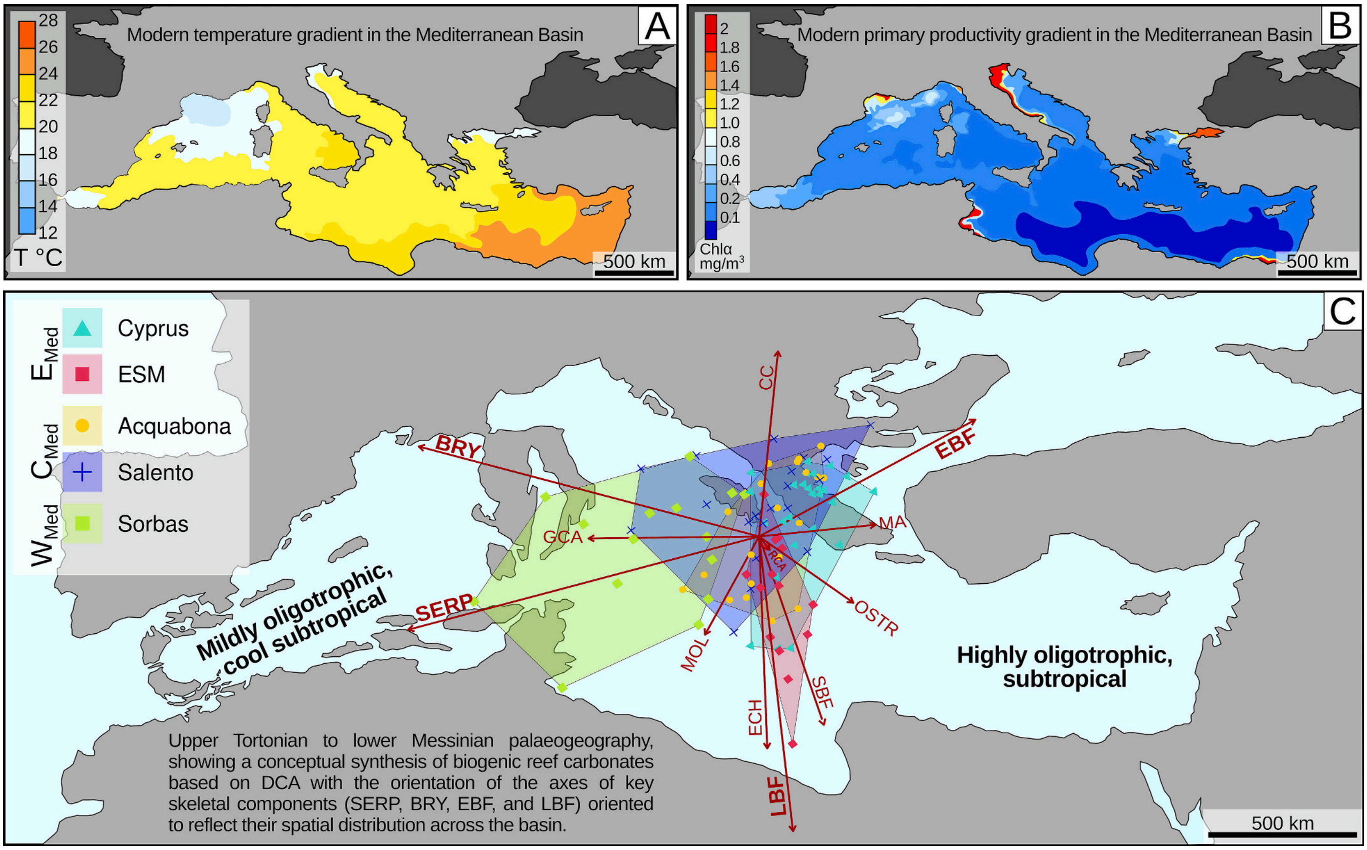

Fig. 9. Environmental gradients in modern and Late Miocene Mediterranean. A) Modern temperature gradient in the Mediterranean Sea based on annual average Sea Surface Temperature is based upon MODIS-Aqua data for the year 2024, downloaded from GIOVANNI, Nasa, (Acker and Leptoukh, 2007). B) Modern primary productivity gradient in the Mediterranean Sea based upon annual average chlorophyll α concentrations from MODIS-Aqua data for the year 2024, downloaded from GIOVANNI, Nasa, (Acker and Leptoukh, 2007). C) Postulated environmental gradient in the Mediterranean during the late Tortonian to early Messinian as suggested by the quantitative analysis of carbonate producers. The late Tortonian to early Messinian palaeogeography is here presented alongside a conceptual synthesis of the analysed reef carbonates. This synthesis, derives from DCA focused on coral-rich facies (Fig. 6B), one of the analysis where the pattern highlighted in the discussion can be clearly seen. It is placed in the centre of the basin for the purpose of visualization (the position of the plot is schematic and not geographically accurate, although it effectively illustrates the main gradients across the Mediterranean area). It features axes for some key components (SERP, BRY, EBF, and LBF) oriented to reflect their spatial distribution across the basin as discussed in the text. The palaeogeographic map integrates the late Tortonian reconstructions of Dercourt et al. (2000) and the Tortonian palaeogeographies of Perrin and Bosellini (2012). The connection with the Atlantic Ocean is based on the detailed reconstruction by Roveri et al. (2025) for the late Tortonian–early Messinian interval. This time interval is considered the most representative for the entire dataset, which incorporates sites from across the Western, Central, and Eastern Mediterranean. (For interpretation of the references to colour in this figure legend, the reader is referred to the web version of this article.)

baselines, with the Western Mediterranean being, on average, cooler and more nutrient-rich than the Eastern Mediterranean.

5.3. Quantitative analysis as a tracker of environmental gradients

As discussed in previous paragraphs, the presence/absence analysis, based on the low presence of green calcareous algae, suggests that the investigated Upper Miocene Mediterranean carbonate systems developed in subtropical conditions. However, this analysis does not allow for a clear inference of environmental gradients across the basin. The relative abundance of LBF, as tracked through quantitative analysis, is suggestive of a WNW–ESE temperature gradient. The ordination plots also highlight a larger relevance of heterotrophs in the western site than in the eastern sites, with the central sites displaying intermediate conditions (Figs. 5–8), consistent with a gradient of increasing nutrients and/or reduced temperatures moving from ESE to WNW (Fig. 9). Both the temperature and the nutrient gradients still exist today in the Mediterranean (Antoine et al., 1995; Basso et al., 2004; Bosc et al., 2004; Pastor et al., 2019) (Fig. 9).

The quantitative analysis is, however, subject to certain limitations. The investigated sites are not coeval but somewhat scattered between the late Tortonian and the pre-evaporitic Messinian (i.e., roughly from 8.5 to 6.7 Ma) (Martín and Braga, 1994; Bossio et al., 1996; Bosellini et al., 2001, 2002; Reolid et al., 2017a, 2017b; Coletti et al., 2019, 2021; Cannings et al., 2021, 2025). During this time, environmental conditions may have changed, potentially influencing the results. This issue is typical of palaeoenvironmental studies based on shallow-marine deposits as they lack, more often than not, abundant planktonic taxa useful for accurate biostratigraphic correlations. However, while time accuracy remains an issue, large-scale reconstructions indicate that during the investigated interval, comprised from around 8 Ma and 6.7 Ma (i.e., the beginning of the “start phase” sensu Corbí et al., 2020), the climate remained reasonably stable (Böhme et al., 2011; Prista et al., 2015; Westerhold et al., 2020). The overall palaeocirculation in the basin also remained mostly unchanged during this period of time, with the Atlantic gateway(s) serving as the primary connection between the Mediterranean and the rest of the oceans (e.g., Capella et al., 2019). Although remarkable changes are known to have occurred in the 500 kyr preceding the MSC, including relevant fluxes of freshwater from Paratethys and African rivers (Vasiliev et al., 2019), the overall boundary conditions to the Mediterranean Basin during the interval comprised between the late Tortonian and the initial phase of the Messinian Salinity Crisis, should have remained sufficiently stable to not jeopardize the significance of the results.

The second problem is related to the representativeness of the investigated samples, i.e., are the examined samples indicative of the whole system? Carbonate systems are complex and their overall variability is challenging to asses (Pomar and Hallock, 2008; Brandano et al., 2022). However, rather than relying on average values alone, which are inherently sensitive to the number of samples collected in each facies, this study reconstructs the Late Miocene palaeo-gradient by analysing the placement of site-specific clusters within the ordination space (i.e., the extent to which a cluster shifts towards a specific group of carbonate producers). These clusters serve as reliable proxies for system-wide variability, as they comprise samples systematically collected from every facies type of the investigated systems according to the established geological knowledge. The robustness of the resulting analysis is testified by the consistency of the patterns emerging across various analytical configurations, including those based only on subsets of the database (Figs. 5–8).

Finally, while the influence of local effects cannot be entirely ruled out, this potential bias is mitigated by focusing on the overall variability of the skeletal assemblages rather than on their average compositions, as well as by analysing a wide range of samples from diverse facies and multiple localities within the same carbonate system.

Notwithstanding the aforementioned limitations, the quantitative analysis of the skeletal assemblages manages to provide more information than the presence/absence approach, successfully capturing a relevant large-scale environmental gradient that proved elusive even when using biodiversity databases. Indeed, to further test the strength of the quantitative microfacies approach against one based solely on presence/absence data, our results are compared with those of another study encompassing the entire Mediterranean (Agiadi et al., 2024a, 2024b). Agiadi et al. (2024a, 2024b) uses time frames of similar length or longer (e.g. the whole Tortonian) and fossil biodiversity data (therefore presence/absence data) to assess the impact of the MSC. Their analysis highlighted a southeastward-decreasing gradient in species richness in the Zanclean, but not in the Tortonian. The Zanclean ecological gradient is consistent with what is observed today as a function of the distance from the Atlantic gateway at Gibraltar (Coll et al., 2010). However, because the palaeoceanographic configuration of the Tortonian Mediterranean Sea already featured the Atlantic Ocean as the main source of biodiversity, such a gradient was expected to have already been established by the Late Miocene (Agiadi et al., 2024a, 2024b). Thus, Agiadi et al. (2024a) concluded that the post-MSC biodiversity gradient may reflect a complex combination of environmental factors rather than the mere effect of distance from its Atlantic ingression point. However, there are reasons to think that the biodiversity patterns outlined by Agiadi et al. (2024a) could also stem from the biogeographic legacy of the Neogene Mediterranean Sea in addition to the basin's changing environmental gradients. Indeed, the pre-MSC Mediterranean was essentially a remnant of the western Tethys Ocean that had happened to detach from its eastern counterpart while remaining connected with the Atlantic realm and, intermittently, with the Paratethys (Bialik et al., 2019; Vasiliev et al., 2019). As a consequence of this, Late Miocene Mediterranean biocoenoses were comprised of complex mixtures of Tethys- and Atlantic-derived forms as well as of a minority of native endemics (Agiadi et al., 2024a, 2024b). After the MSC, during the earliest Pliocene, a fully marine Mediterranean Sea was restored – one that was still home to some Miocene survivors (e.g., Collareta et al., 2021), including shrinking numbers of Tethys-derived relicts. If the Mediterranean ecosystems were largely reset during the MSC, then the modern eastward-decreasing richness gradient may have been established during the Zanclean as a by-product of such a reset, which abruptly diminished the influence of the basin's past as one of the many sectors of the much larger, biodiversity-rich Tethys Ocean.

Therefore, three hypothetical scenarios may thus account for the biodiversity patterns observed in the Late Miocene Mediterranean Sea: 1) the WNW–ESE environmental gradient had not yet developed, and as such, it left no signal in palaeobiodiversity analyses; 2) the gradient was already established and influenced the Mediterranean biodiversity, but its imprint could not be captured because of the inherent limitations of presence/absence databases; 3) the gradient existed, but its influence on biodiversity was overshadowed by the basin's biogeographic legacy, rendering it again undetectable in palaeobiodiversity analyses. Given the palaeoceanographic framework of the Late Miocene Mediterranean, the existence of a WNW–ESE environmental gradient is strongly expected, making the first scenario the least plausible. Consequently, the argument reduces to the second and third scenarios, both of which point to quantitative microfacies analysis as a more reliable tool than presence/absence analysis for identifying large-scale paleoenvironmental gradients.

5.4. Late Miocene Mediterranean reef and reef-related carbonate factories

Thanks to quantitative microfacies analysis, the current study can help fill in the gaps in presence/absence and biodiversity analyses, providing new insights into Late Miocene reef-bearing, shallow-water carbonate systems.

The investigated upper Tortonian to pre-evaporitic Messinian coral-rich carbonate factories were likely similar to those occurring today in oligotrophic subtropical conditions, i.e., largely dominated by red calcareous algae and symbiont-bearing colonial corals. Unlike modern reefs, encrusting benthic foraminifera (particularly nubeculariids) were often the third most relevant carbonate producers. Close to the reef, bioclastic production by molluscs, small benthic foraminifera (mainly *Elphidium* and small porcellaneous taxa), *Halimeda*, and echinoderms was relevant. Large benthic foraminifera (mainly *Dentritina* and *Borelis*) were only occasionally abundant in lagoonal settings. Serpulids and bryozoans were present in both reefs and reef-related settings, albeit as minor components, providing a more relevant contribution wherever nutrient availability was higher and light availability lower. These carbonate factories likely represented an adaptation of "modern-like" reef factories to relatively cool but often highly oligotrophic subtropical conditions. These factories likely remained relatively stable, with some reduction in biodiversity (Bosellini and Perrin, 2008; Perrin and Bosellini, 2012), up until around 500 kyr before the onset of the MSC (Vasiliev et al., 2019). After this point, the restriction of the basin resulted into more stressful conditions, culminating in the MSC. This is reflected in the uppermost portion of Upper Miocene shallow-water successions and particularly in Terminal Carbonate Complexes. The latter differs from the investigated reef carbonates by a more relevant and pervasive contribution of microbial carbonate production and the abundance of oolites (Esteban, 1979; Riding et al., 1991; Martín et al., 1993; Kolodka et al., 2016; Vescogni et al., 2022, 2025; Vescogni and Guido, 2026).

6. Conclusions

The current basin-wide analysis of Upper Miocene shallow-water, reef-bearing carbonate successions confirms the subtropical character of these environments, in agreement with previous studies. However, it expands upon previous literature thanks to its comprehensive dataset of skeletal assemblages. Both presence/absence and quantitative analyses indeed indicate a subtropical setting, but, only the quantitative approach successfully captures the environmental gradients across the basin.

The relative abundance of large benthic foraminifera emerges as a potential indicator of temperature variation, whereas bryozoans and serpulids are likely more sensitive to nutrient availability. Fossil nubeculariid encrusting benthic foraminifera (characterised by the development of thick crusts) appear instead to reflect shallow, warm, and potentially stressful conditions with limited water circulation. All observations collectively are consistent with a WNW–ESE gradient of decreasing nutrient availability and increasing temperature. This result is in agreement with present-day Mediterranean environments and the overall palaeogeographic context during most of the Late Miocene, during which the Atlantic became the only remaining connection with the global oceans.

The quantitative study of the skeletal assemblages, paired with ordination analysis, proved to be more effective than presence/absence and biodiversity-based approaches in detecting this basin-wide environmental patterns. This quantitative approach facilitates the establishment of a general framework within which other Upper Miocene reefs of the Mediterranean can be studied and compared. Ultimately, this will further our knowledge of the last major chapter of the Mediterranean's tropical history, providing precious insights into the next one, currently unfolding due to the ongoing re-tropicalisation of the basin.

CRediT authorship contribution statement

Giovanni Coletti: Writing – review & editing, Writing – original draft, Visualization, Validation, Supervision, Methodology, Investigation, Formal analysis, Data curation, Conceptualization. **Alberto Vimercati:** Writing – review & editing, Writing – original draft, Visualization, Software, Methodology, Investigation, Formal analysis, Conceptualization. **Francesca R. Bosellini:** Writing – review & editing, Writing – original draft, Supervision, Investigation, Formal analysis. **Luca Mariani:** Writing – review & editing, Investigation, Conceptualization. **Adriano Guido:** Writing – review & editing, Writing – original draft, Investigation. **Alessandro Vescogni:** Writing – review & editing, Writing – original draft, Investigation. **Jesús Reolid:** Writing – review & editing, Writing – original draft, Investigation. **Gerald Auer:** Writing – review & editing, Investigation, Conceptualization. **Daniela Basso:** Writing – review & editing, Supervision. **Alberto Collareta:** Writing – review & editing, Investigation, Conceptualization. **Giulia Bosio:** Writing – review & editing, Investigation, Conceptualization. **Or Mordecai Bialik:** Writing – review & editing, Writing – original draft, Visualization, Supervision, Methodology, Investigation, Conceptualization.

Declaration of competing interest

The authors declare that they have no known competing financial interests or personal relationships that could have appeared to influence the work reported in this paper.

Acknowledgments

The authors wish to express their sincere gratitude to the Italian Palaeontological Society (SPI) and the International Association of Sedimentologists (IAS) for fostering the scientific environment from which this research originated. We are also deeply thankful to Alastair Robertson and Elizabeth Balmer for their long-standing support and valuable assistance in studying and interpreting the geology and stratigraphy of Cyprus.

The authors would also like to thank Prof. Guillem Mateu-Vicens and the editorial board of the journal for their helpful suggestions and comments that significantly improved the manuscript. Finally, G.C. and D.B. wish to dedicate a special acknowledgment to the late Silvia Spezzaferri, whose remarkable ability to connect people and inspire scientific collaboration lies at the heart of this work. Without her vision and generosity, this and many other studies would not have come to fruition.

This research did not receive any specific grant from funding agencies in the public, commercial, or not-for-profit sectors, its results represents a scientific contribution to Project MIUR - Dipartimenti di Eccellenza 2023–2026.

Appendix A. Supplementary data

Supplementary data to this article can be found online at https://doi.org/10.1016/j.palaeo.2026.114023.

Data availability

The authors confirm that all data necessary for supporting the scientific findings of this paper have been provided.

References

Acker, J.G., Leptoukh, G., 2007. Online analysis enhances use of NASA Earth Science data. Eos. Trans. AGU 88 (2), 14–17.

Agiadi, K., Hohmann, N., Gliozzi, E., Thivaiou, D., Bosellini, F.R., Taviani, M., Bianucci, G., Collareta, A., Londeix, L., Faranda, C., Bulian, F., Koskeridou, E., Lozar, F., Mancini, A.M., Dominici, S., Moissette, P., Bajo Campos, I., Borghi, E., Iliopoulos, G., Antonarakou, A., Kontakiotis, G., Besiou, E., Zarkogiannis, S.D., Harzhauser, M., Sierro, F.J., Coll, M., Vasiliev, I., Camerlenghi, A., García-Castellanos, D., 2024a. The marine biodiversity impact of the late Miocene Mediterranean salinity crisis. Science 385 (6712), 986–991.

Agiadi, K., Hohmann, N., Gliozzi, E., Thivaiou, D., Bosellini, F.R., Taviani, M., Bianucci, G., Collareta, A., Londeix, L., Faranda, C., Bulian, F., Koskeridou, E., Lozar, F., Mancini, A.M., Dominici, S., Moissette, P., Bajo Campos, I., Borghi, E., Iliopoulos, G., Antonarakou, A., Kontakiotis, G., Besiou, E., Zarkogiannis, S.D., Harzhauser, M., Sierro, F.J., Coll, M., Vasiliev, I., Camerlenghi, A., García-Castellanos, D., 2024b. Late Miocene transformation of Mediterranean Sea biodiversity. Sci. Adv. 10 (39), eadp1134.

Aguirre, J., Riding, R., Braga, J.C., 2000. Late cretaceous incident light reduction: evidence from benthic algae. Lethaia 33 (3), 205–213.

Aktaş, G., Robertson, A.H.F., 1984. The Maden complex, SE Turkey: Evolution of a Neotethyan active margin. In: Dixon, J.E., Robertson, A.H.F. (Eds.), The Geological Evolution of the Eastern Mediterranean, 17. Geol. Soc. Spec. Publ., pp. 375–402

Alós, J., Tomas, F., Terrados, J., Verbruggen, H., Ballesteros, E., 2016. Fast-spreading green beds of recently introduced *Halimeda incrassata* invade Mallorca island (NW Mediterranean Sea). Mar. Ecol. Prog. Ser. 558, 153–158.

Anderson, M.J., 2014. Permutational Multivariate Analysis of Variance (PERMANOVA). Wiley StatsRef: Statistics Reference Online, pp. 1–15.

Antoine, D., Morel, A., André, J.M., 1995. Algal pigment distribution and primary production in the eastern Mediterranean as derived from Coastal Zone Color Scanner observations. J. Geophys. Res. Oceans 100 (C8), 16193–16209.

Anton, A., Randle, J.L., Garcia, F.C., Rossbach, S., Ellis, J.I., Weinzierl, M., Duarte, C.M., 2020. Differential thermal tolerance between algae and corals may trigger the proliferation of algae in coral reefs. Glob. Chang. Biol. 26 (8), 4316–4327.

Basso, D., Corselli, C., 2002. Community versus biocoenosis in multivariate analysis of benthic molluscan thanatocoenoses. Riv. Ital. Paleontol. Stratigr. 108 (1).

Basso, D., Thomson, J., Corselli, C., 2004. Indications of low macrobenthic activity in the deep sediments of the eastern Mediterranean Sea. Sci. Mar. 68 (S3), 53–62.

Bastos, A.C., Moura, R.L., Moraes, F.C., Vieira, L.S., Braga, J.C., Ramalho, L.V., Amado-Filho, G.M., Magdalena, U.R., Webster, J.M., 2018. Bryozoans are major modern builders of South Atlantic oddly shaped reefs. Sci. Rep. 8 (1), 9638.

Beavington-Penney, S.J., Racey, A., 2004. Ecology of extant nummulitids and other larger benthic foraminifera: applications in palaeoenvironmental analysis. Earth Sci. Rev. 67 (3–4), 219–265.

Benedetti, A., Papazzoni, C.A., Bosellini, F.R., 2024. Unparallel resilience of shallow-water tropical calcifiers (foraminifera and scleractinian reef corals) during the early Paleogene global warming intervals. Palaeogeogr. Palaeoclimatol. Palaeoecol. 651, 112393.

Bialik, O.M., Frank, M., Betzler, C., Zammit, R., Waldmann, N.D., 2019. Two-step closure of the Miocene Indian Ocean Gateway to the Mediterranean. Sci. Rep. 9, 8842.

Bialik, O.M., Jarochowska, E., Grossowicz, M., 2021a. Ordination analysis in sedimentology, geochemistry and palaeoenvironment—Background, current trends and recommendations. Depositional Rec. 7 (3), 541–563.

Bialik, O.M., Zammit, R., Micallef, A., 2021b. Architecture and sequence stratigraphy of the Upper Coralline Limestone formation, Malta—Implications for Eastern Mediterranean restriction prior to the Messinian Salinity Crisis. Depositional Rec. 7 (2), 256–270.

Bialik, O.M., Reolid, J., Kulhanek, D.K., Hincke, C., Waldmann, N.D., Betzler, C., 2022. Sedimentary response to current and nutrient regime rearrangement in the Eastern Mediterranean during the early to middle Miocene (SW Cyprus). Palaeogeogr. Palaeoclimatol. Palaeoecol. 588, 110819.

Bialik, O.M., Coletti, G., Mariani, L., Commissario, L., Desbiolles, F., Meroni, A.N., 2023. Availability and type of energy regulate the global distribution of neritic carbonates. Sci. Rep. 13, 19687.

Böhme, M., Winklhofer, M., Ilg, A., 2011. Miocene precipitation in Europe: Temporal trends and spatial gradients. Palaeogeogr. Palaeoclimatol. Palaeoecol. 304 (3–4), 212–218.

Bosc, E., Bricaud, A., Antoine, D., 2004. Seasonal and interannual variability in algal biomass and primary production in the Mediterranean Sea, as derived from 4 years of SeaWiFS observations. Glob. Biogeochem. Cycles 18 (1).

Bosellini, F.R., 2006. Biotic changes and their control on Oligocene-Miocene reefs: a case study from the Apulia Platform margin (southern Italy). Palaeogeogr. Palaeoclimatol. Palaeoecol. 241 (3–4), 393–409.

Bosellini, F.R., Perrin, C., 2008. Estimating Mediterranean Oligocene–Miocene sea-surface temperatures: an approach based on coral taxonomic richness. Palaeogeogr. Palaeoclimatol. Palaeoecol. 258 (1–2), 71–88.

Bosellini, A., Bosellini, F.R., Colalongo, M.L., Parente, M., Russo, A., Vescogni, A., 1999. Stratigraphic architecture of the Salento coast from Capo d'Otranto to S. Maria di Leuca (Apulia, southern Italy). Riv. Ital. Paleontol. Stratigr. 105, 397–416.

Bosellini, F.R., Russo, A., Vescogni, A., 2001. Messinian reef-building assemblages of the Salento Peninsula (southern Italy): palaeobathymetric and palaeoclimatic significance. Palaeogeogr. Palaeoclimatol. Palaeoecol. 175 (1–4), 7–26.

Bosellini, F.R., Russo, A., Vescogni, A., 2002. The Messinian reef complex of the Salento Peninsula (southern Italy): stratigraphy, facies and paleoenvironmental interpretation. Facies 47, 91–112.

Bosellini, F.R., Benedetti, A., Kiessling, W., 2025. Minor coral diversity loss but long-lasting coral reef crises in the early Paleogene hothouse. Paleoceanogr. Paleoclimatol. 40 (3), e2024PA004985.

Bosence, D.W.J., 1973. Recent serpulid reefs, Connemara, Eire. Nature 242 (5392), 40–41.

Bossio, A., Costantini, A., Lazzarotto, A., Liotta, D., Mazzanti, R., Mazzei, R., Salvatorini, G., Sandrelli, F., 1993. Rassegna delle conoscenze sulla stratigrafia del neoautoctono toscano. Mem. Soc. Geol. Ital. 49, 17–98.

Bossio, A., Esteban, M., Mazzanti, R., Mazzei, R., Salvatorini, G., 1996. Rosignano Reef Complex (Messinian), Livornesi Mountains, Tuscany, Central Italy.

Brachert, T.C., Betzler, C., Braga, J.C., Martin, J.M., 1998. Microtaphofacies of a warm-temperate carbonate ramp (uppermost Tortonian/lowermost Messinian, southern Spain). Palaios 13 (5), 459–475.

Braga, J.C., Martin, J.M., 1996. Geometries of reef advance in response to relative sea-level changes in a Messinian (uppermost Miocene) fringing reef (Cariatiz reef, Sorbas Basin, SE Spain). Sediment. Geol. 107 (1–2), 61–81.

Braga, J.C., Martín, J.M., Riding, R., 1996. Internal structure of segment reefs: *Halimeda* algal mounds in the Mediterranean Miocene. Geology 24, 35–38.

Braga, J.C., Vescogni, A., Bosellini, F.R., Aguirre, J., 2009. Coralline algae (Corallinales, Rhodophyta) in western and Central Mediterranean Messinian reefs. Palaeogeogr. Palaeoclimatol. Palaeoecol. 275 (1–4), 113–128.

Brandano, M., Frezza, V., Tomassetti, L., Pedley, M., Matteucci, R., 2009. Facies analysis and palaeoenvironmental interpretation of the late Oligocene Attard Member (lower Coralline Limestone Formation). Malta. Sedimentology 56 (4), 1138–1158.

Brandano, M., Westphal, H., Mateu-Vicens, G., Preto, N., Obrador, A., 2016. Ancient upwelling record in a phosphate hardground (Tortonian of Menorca, Balearic Islands, Spain). Mar. Pet. Geol. 78, 593–605.

Brandano, M., Mateu-Vicens, G., Baceta, J.I., 2022. Understanding carbonate factories through palaeoecological and sedimentological signals–Tribute to Luis Pomar. Sedimentology 69 (1), 5–23.

Bray, J.R., Curtis, J.T., 1957. An ordination of the upland forest communities of Southern Wisconsin. Ecol. Monogr. 27 (4), 325–349.

Buchbinder, B., 1996. Miocene carbonates of the Eastern Mediterranean, the Red Sea and the Mesopotamian Basin: geodynamic and eustatic controls. In: Franseen, E.K., Esteban, M., Ward, W.C., Rouchy, J.M. (Eds.), Models for carbonate stratigraphy, from Miocene reef complex of the Mediterranean regions. Concepts in Sedimentology and Paleontology, Volume 5, pp. 89–96. Tulsa, OK.

Cahuzac, B., Poignant, A., 1997. Essai de biozonation de l'Oligo-Miocène dans les bassins européens à l'aide des grands foraminifères néritiques. Bull. Soc. Géol. Fr. 168 (2), 155–169.

Cannings, T., Balmer, E.M., Coletti, G., Ickert, R.B., Kroon, D., Raffi, I., Robertson, A.H.F., 2021. Microfossil and strontium isotope chronology used to identify the controls of Miocene reefs and related facies in NW Cyprus. J. Geol. Soc. Lond. 178 (2) jgs2020-081.

Cannings, T., Robertson, A.H., Kroon, D., 2025. Insights into the Middle–Late Miocene palaeoceanographic development of Cyprus (eastern Mediterranean) from a new δ 18 O and δ 13 C stable isotope composite record. Clim. Past 21 (12), 2501–2523.

Capella, W., Flecker, R., Hernández-Molina, F.J., Simon, D., Meijer, P.T., Rogerson, M., Sierro, F.J., Krijgsman, W., 2019. Mediterranean isolation preconditioning the Earth System for late Miocene climate cooling. Sci. Rep. 9 (1), 3795.

Caracciolo, L., Gramigna, P., Critelli, S., Calzona, A.B., Russo, F., 2013. Petrostratigraphic analysis of a late Miocene mixed siliciclastic–carbonate depositional system (Calabria, Southern Italy): Implications for Mediterranean paleogeography. Sediment. Geol. 284, 117–132.

Carminati, E., Doglioni, C., 2005. Mediterranean tectonics. In: Encyclopedia of. Geology 2, 135–146.

Carminati, E., Lustrino, M., Doglioni, C., 2012. Geodynamic evolution of the central and western Mediterranean: tectonics vs. igneous petrology constraints. Tectonophysics 579, 173–192.

Chen, C.A., 1999. Analysis of scleractinian distribution in Taiwan indicating a pattern congruent with sea surface temperatures and currents: examples from *Acropora* and Faviidae corals. Zool. Stud. 38, 119–129.

Clarke, K.R., Green, R.H., 1988. Statistical design and analysis for a 'biological effects' study. Mar. Ecol. Prog. Ser. 213–226.

Coletti, G., Basso, D., 2020. Coralline algae as depth indicators in the Miocene carbonates of the Eratosthenes Seamount (ODP Leg 160, Hole 966F). Geobios 60, 29–46.

Coletti, G., Bracchi, V., Corselli, C., Marchese, F., Basso, D., Savini, A., Vertino, A., 2018. Quaternary build-ups and rhodalgal carbonates along the Adriatic and Ionian coasts of the Italian Peninsula: a review. Riv. Ital. Paleontol. Stratigr. 124 (1), 387–406.

Coletti, G., Basso, D., Betzler, C., Robertson, A.H.F., Bosio, G., El Kateb, A., Foubert, A., Meilijson, A., Spezzaferri, S., 2019. Environmental evolution and geological significance of the Miocene carbonates of the Eratosthenes Seamount (ODP Leg 160). Palaeogeogr., Palaeoclimatol. Palaeoecol 530, 217–235.

Coletti, G., Balmer, E.M., Bialik, O.M., Cannings, T., Kroon, D., Robertson, A.H.F., Basso, D., 2021. Microfacies evidence for the evolution of Miocene coral-reef environments in Cyprus. Palaeogeogr. Palaeoclimatol. Palaeoecol. 584, 110670.

Coletti, G., Commissario, L., Mariani, L., Bosio, G., Desbiolles, F., Soldi, M., Bialik, O.M., 2022. Palaeocene to Miocene southern Tethyan carbonate factories: a meta-analysis of the successions of south-western and western Central Asia. Depositional Rec. 8 (3), 1031–1054.

Coletti, G., Vimercati, A., Bosellini, F.R., Collareta, A., Bosio, G., Guido, A., Vescogni, A., Basso, D., Bialik, O.M., 2024. Dancing towards the end—Ecological oscillations in Mediterranean coral reefs prior to the Messinian Salinity Crisis (Calcare di Rosignano Formation, Acquabona, Tuscany, Italy). Geosciences 14 (11), 285.

Coll, M., Piroddi, C., Steenbeek, J., Kaschner, K., Ben Rais Lasram, F., Aguzzi, J., Ballesteros, E., Bianchi, C.N., Corbera, J., Dailianis, T., Danovaro, R., Estrada, M., Froglia, C., Galil, B.S., Gasol, J.M., Gertwagen, R., Gil, J., Guilhaumon, F., Kesner-Reyes, K., Kitsos, M.-S., Koukouras, A., Lampadariou, N., Laxamana, E., López-Fé de la Cuadra, C.M., Lotze, H.K., Martin, D., Mouillot, D., Oro, D., Raicevich, S., Rius-Barile, J., Saiz-Salinas, J.I., San Vicente, C., Somot, S., Templado, J., Turon, X., Vafidis, D., Villanueva, R., Voultsiadou, E., 2010. The biodiversity of the Mediterranean Sea: estimates, patterns, and threats. PLoS One 5 (8), e11842.

Collareta, A., Merella, M., Casati, S., Coletti, G., Di Cencio, A., 2021. Another thermophilic" Miocene survivor" from the Italian Pliocene: A geologically young occurrence of the pelagic eagle ray Aetobatus in the Euro-Mediterranean region. Carnets de Geologie 21 (10), 203–214.

Corbí, H., Soria, J.M., Giannetti, A., Yébenes, A., 2020. The step-by-step restriction of the Mediterranean (start, amplification, and consolidation phases) preceding the Messinian Salinity Crisis (climax phase) in the Bajo Segura basin. Geo-Mar. Lett. 40 (3), 341–361.

Cornacchia, I., Andersson, P., Agostini, S., Brandano, M., Di Bella, L., 2017. Strontium stratigraphy of the upper Miocene Lithothamnion Limestone in the Majella

Mountain, Central Italy, and its palaeoenvironmental implications. Lethaia 50 (4), 561–575.
Cornacchia, I., Agostini, S., Brandano, M., 2018. Miocene oceanographic evolution based on the Sr and Nd isotope record of the Central Mediterranean. Paleoceanograph. Paleoclimatol. 33 (1), 31–47.
Cornacchia, I., Brandano, M., Agostini, S., 2021. Miocene paleoceanographic evolution of the Mediterranean area and carbonate production changes: A review. Earth Sci. Rev. 221, 103785.
Cornacchia, I., Catanzariti, R., Di Marcantonio, E., Mancini, A., Carpenito, F., Brandano, M., 2026. Central Mediterranean progressive isolation and climate change from Tortonian to early Messinian: insight from hemipelagic successions of Central Apennines (Central Italy). Palaeogeogr. Palaeoclimatol. Palaeoecol. this volume.
Dercourt, J., Gaetani, M., Vrielynk, B., Barrier, E., Biju-Duval, B., Brunet, M.F., Cadet, J. P., Crasquin, S., Sandulescu, M., 2000. Atlas Peri-Tethys. Palaeogeographical maps, p. 279.
Di Credico, N., Fravega, P., Giammarino, S., Piazza, M., Vannucci, G., 2004. Algal assemblages of Cala Pisana Member, Lampedusa Formation (late Miocene, Lampedusa Island). Boll. Acc. Gioenia Sci. Nat 37, 217–243.
Eaton, S., Robertson, A.H.F., 1993. The Miocene Pakhna Formation, southern Cyprus and its relationship to the Neogene tectonic evolution of the Eastern Mediterranean. Sediment. Geol. 86, 273–296.
Esteban, M., 1979. Significance of the upper Miocene coral reefs of the western Mediterranean. Palaeogeogr., Palaeoclimatol. Palaeoecol 29, 169–188.
Esteban, M., 1996. An overview of Miocene reefs from Mediterranean areas: General trends and facies models. In: Franseen, E.K., Esteban, M., Ward, W.C., Rouchy, J.M. (Eds.), Models for Carbonate Stratigraphy, from Miocene Reef Complex of the Mediterranean Regions, Concepts in Sedimentology and Paleontology Volume 5. Tulsa, OK, pp. 3–53.
Faccenna, C., Piromallo, C., Crespo-Blanc, A., Jolivet, L., Rossetti, F., 2004. Lateral slab deformation and the origin of the western Mediterranean arcs. Tectonics 23 (1).
Flügel, E., Kiessling, W., 2002. Patterns of Phanerozoic reef crises. Earth Sci. Rev. 58, 1–74.
Follows, E.J., 1992. Patterns of reef sedimentation and diagenesis in the Miocene of Cyprus. Sediment. Geol. 79 (1–4), 225–253.
Follows, E.J., Robertson, A.H.F., 1990. Sedimentology and structural setting of Miocene reefal limestone in Cyprus. In: Panayiotou, A. (Ed.), Ophiolites: Oceanic Crustal Analogues, Geol. Surv. Dep, Nicosia, pp. 207–216.
Follows, E.J., Robertson, A.H., Scoffin, T.P., 1996. Tectonic controls on Miocene reefs and related carbonate facies in Cyprus. Sediment. Geol. 103, 25–46.
Fornós, J.J., Forteza, V., Martínez-Taberner, A., 1997. Modern polychaete reefs in western Mediterranean lagoons: *Ficopomatus enigmaticus* (Fauvel) in the Albufera of Menorca, Balearic Islands. Palaeogeogr. Palaeoclimatol. Palaeoecol. 128 (1–4), 175–186.
Fravega, P., Piazza, M., Vannucci, G., 1994. Nongeniculate coralline algae associations from the Calcare di Rosignano Formation, lower Messinian, Tuscany (Italy). In: Matteucci, R. (Ed.), Studies on ecology and paleoecology of benthic communities, Bollettino Soc. Paleontol. Ital. Spec. Vol. 2, 127–140.
Gauch, H.G., Whittaker, R.H., 1972. Comparison of ordination techniques. Ecology 53 (5), 868–875.
Gramigna, P., Bassi, D., Russo, F., 2012. An upper Miocene siliciclastic-carbonate ramp: depositional architecture, facies distribution, and diagenetic history (Capo Vaticano area, southern Italy). Facies 58 (2), 191–215.
Granier, B., 2012. The contribution of calcareous green algae to the production of limestones: a review. Geodiversitas 34 (1), 35–60.
Granier, B.R., 2024. Reassessment of *Iberopora bodeuri*, a primitive plurilocular calcareous encrusting foraminifer from the “Upper Jurassic” (including Berriasian) carbonate platforms of the northern and central Tethys. Cretac. Res. 155, 105782.
Guerra-Merchán, A., Serrano, F., 1993. Tectosedimentary setting and chronostratigraphy of the Neogene reefs in the Almanzora Corridor (Betic Cordillera, Spain). Geobios 26 (1), 57–67.
Guido, A., Mastandrea, A., Stefani, M., Russo, F., 2016. Role of autochthonous versus detrital micrite in depositional geometries of Middle Triassic carbonate platform systems. GSA Bull. 128, 989–999.
Guido, A., Palladino, G., Sposato, M., Russo, F., Prosser, G., Bentivenga, M., Mastandrea, A., 2021. Reconstruction of tectonically disrupted carbonates through quantitative microfacies analyses: an example from the Middle Triassic of Southern Italy. Facies 67, 22.
Hill, M.O., 1979. Decorana—A Fortran Program for Detrended Correspondence Analysis and Reciprocal Averaging. Cornell Univ, Section of Ecology and Systematics.
Hsü, K.J., Ryan, W.B.F., Cita, M.B., 1973. Late Miocene dessiccation of the Mediterranean. Nature 242, 240–244.
Johnson, K.G., Jackson, J.B.C., Budd, A.F., 2008. Caribbean reef development was independent of coral diversity over 28 million years. Science 319, 1521–1523.
Jost, L., Chao, A., Chazdon, R.L., 2011. Compositional similarity and β (beta) diversity. In: Magurran, A.E., McGill, B.J. (Eds.), Biological Diversity: Frontiers in Measurement and Assessment. Oxford Univ, Press, pp. 66–84.
Khen, A., Johnson, M.D., Fox, M.D., Smith, J.E., 2025. Benthic algal community dynamics on Palmyra Atoll throughout a decade with two thermal anomalies. Front. Mar. Sci. 12, 1539865.
Kiessling, W., Flügel, E., Golonka, J., 1999. Paleoreef maps: evaluation of a comprehensive database on Phanerozoic reefs. AAPG Bull. 83, 1552–1587.
Kinnaird, T., Robertson, A.H.F., 2013. Tectonic and sedimentary response to subduction and incipient collision in southern Cyprus, easternmost Mediterranean region. In: Robertson, A.H.F., Parlak, O., Ünlügenç, U.C. (Eds.), Geological Development of Anatolia and the Easternmost Mediterranean Region. Geol. Soc. London. Spec. Publ. 372, 585–614.
Kočí, T., Bosio, G., Collareta, A., Sanfilippo, R., Ekrt, B., Urbina, M., Malinverno, E., 2021. First report on the cirratulid (Annelida, Polychaeta) reefs from the Miocene Chilcatay and Pisco Formations (East Pisco Basin, Peru). J. S. Am. Earth Sci. 107, 103042.
Kolodka, C., Vennin, E., Bourillot, R., Granjeon, D., Desaubliaux, G., 2016. Stratigraphic modelling of platform architecture and carbonate production: a Messinian case study (Sorbas Basin, SE Spain). Basin Res. 28, 658–684.
Kruskal, J.B., 1964. Nonmetric multidimensional scaling: a numerical method. Psychometrika 29, 115–129.
Legendre, P., Borcard, D., 2018. Box–Cox–chord transformations for community composition data prior to beta diversity analysis. Ecography 41, 1820–1824.
Legendre, P., Gallagher, E.D., 2001. Ecologically meaningful transformations for ordination of species data. Oecologia 129, 271–280.
MacKenzie, D.I., 2005. Was it there? Dealing with imperfect detection for species presence/absence data. Aust. N. Z. J. Stat. 47, 65–74.
MacKenzie, D.I., Nichols, J.D., Lachman, G.B., Droege, S., Royle, J.A., Langtimm, C.A., 2002. Estimating site occupancy rates when detection probabilities are less than one. Ecology 83, 2248–2255.
Mariani, L., Coletti, G., Bosio, G., Mateu-Vicens, G., Ali, M., Cavallo, A., Mittempergher, S., Malinverno, E., 2024. Tectonically-controlled biofacies distribution in the Eocene Foraminiferal Limestone (Pag, Croatia): A quantitative-based palaeontological analysis. Sediment. Geol. 472, 106743.
Mariani, L., Coletti, G., Vescogni, A., Vimercati, A., Bosellini, F.R., 2026. Skeletal assemblage fluctuations within persistent Mediterranean coral-reef framework during Cenozoic warming events. Sediment. Geol. 501, 107124.
Marshall, J.F., Davies, P.J., 1988. *Halimeda* bioherms of the northern Great Barrier Reef. Coral Reefs 6, 139–148.
Mart, Y., Robertson, A.H.F., 1998. Eratosthenes Seamount: an oceanographic yardstick recording the late Mesozoic–Tertiary geological history of the Eastern Mediterranean. In: Robertson, A.H.F., Emeis, K.C., Richter, C., Camerlenghi, A. (Eds.), Proc. Ocean Drill. Program, Sci. Results, 160, pp. 701–708.
Martín, J., Braga, J.C., 1994. Messinian events in the Sorbas Basin in southeastern Spain and their implications in the recent history of the Mediterranean. Sediment. Geol. 90, 257–268.
Martín, J.M., Braga, J.C., Riding, R., 1993. Siliciclastic stromatolites and thrombolites, late Miocene, SE Spain. J. Sediment. Res. 63, 131–139.
Martín, J.M., Braga, J.C., Riding, R., 1997. Late Miocene Halimeda alga-microbial segment reefs in the marginal Mediterranean Sorbas Basin. Spain. Sedimentology 44 (3), 441–456.
Martín, J.M., Braga, J.C., Sánchez-Almazo, I.M., Aguirre, J., 2012. Temperate and Tropical Carbonate sedimentation Episodes in the Neogene Betic Basins (Southern Spain) Linked to Climatic Oscillations and changes in Atlantic-Mediterranean Connections: Constraints from Isotopic Data. Carbonate systems during the Oligocene–Miocene climatic transition 49–69.
Martini, I.P., Sagri, M., 1993. Tectono-sedimentary characteristic of Late Miocene–Quaternary extensional basins of the Northern Apennines, Italy. Earth Sci. Rev. 34, 197–233.
Mateu-Vicens, G., Hallock, P., Brandano, M., 2008. A depositional model and paleoecological reconstruction of the lower Tortonian distally steepened ramp of Menorca (Balearic Islands, Spain). Palaios 23 (7), 465–481.
Mateu-Vicens, G., Khokhlova, A., Sebastián-Pastor, T., 2014. Epiphytic foraminiferal indices as bioindicators in Mediterranean seagrass meadows. J. Foraminiferal Res. 44 (3), 325–339.
Mazzanti, R., Bossio, A., Cascella, A., Foresi, M., Mazzei, R., Salvatorini, G., Putignano, M.L., 2016. Note Illustrative della Carta Geologica d'Italia alla scala 1: 50.000, Foglio 284 Rosignano Marittimo. Serv. Geol. d'Italia, ISPRA, Roma, p. 189.
McNeil, M.A., Webster, J.M., Beaman, R.J., Graham, T.L., 2016. New constraints on the spatial distribution and morphology of the Halimeda bioherms of the Great Barrier Reef. Australia. Coral Reefs 35 (4), 1343–1355.
McNeil, M., Firn, J., Nothdurft, L.D., Pearse, A.R., Webster, J.M., Roland Pitcher, C., 2021. Inter-reef *Halimeda* algal habitats within the Great Barrier Reef support a distinct biotic community and high biodiversity. Nature Ecology & Evolution 5 (5), 647–655.
McNeil, M., Nothdurft, L.D., Hua, Q., Webster, J.M., Moss, P., 2022. Evolution of the inter-reef *Halimeda* carbonate factory in response to Holocene Sea-level and environmental change in the Great Barrier Reef. Quat. Sci. Rev. 277, 107347.
Meilijson, A., Hilgen, F., Sepúlveda, J., Steinberg, J., Fairbank, V., Flecker, R., Waldmann, N.D., Spaulding, S.A., Bialik, O.M., Garrett Boudinot, F., Illner, P., Makovsky, Y., 2019. Chronology with a pinch of salt: Integrated stratigraphy of Messinian evaporites in the deep Eastern Mediterranean reveals long-lasting halite deposition during Atlantic connectivity. Earth Sci. Rev. 194, 374–398.
Montefalcone, M., Oprandi, A., Azzola, A., Morri, C., Bianchi, C.N., 2022. Serpulid reefs and their role in aquatic ecosystems: A global review. Adv. Mar. Biol. 92, 1–54.
Mutti, M., Hallock, P., 2003. Carbonate systems along nutrient and temperature gradients: some sedimentological and geochemical constraints. Int. J. Earth Sci. 92, 465–475.
Muttoni, G., Dallanave, E., Channell, J.E.T., 2013. The drift history of Adria and Africa from 280 Ma to present, Jurassic true polar wander, and zonal climate control on Tethyan sedimentary facies. Palaeogeogr. Palaeoclimatol. Palaeoecol. 386, 415–435.
Nooitgedacht, C.W., Kleipool, L.M., Andeweg, B., Reolid, J., Betzler, C., Lindhorst, S., Reijmer, J.J., 2018. New insights in the development of syn-depositional fractures in rimmed flat-topped carbonate platforms, Neogene carbonate complexes, Sorbas Basin. SE Spain. Basin Res. 30, 596–612.
Obrador, A., Pomar, L., Taberner, C., 1992. Late Miocene breccia of Menorca (Balearic Islands) a basis for the interpretation of a Neogene ramp deposit. Sediment. Geol. 79 (1–4), 203–223.

Pandolfi, J.M., Kiessling, W., 2014. Gaining insights from past reefs to inform understanding of coral reef response to global climate change. Curr. Opin. Environ. Sustain. 7, 52–58.

Passaseo, C., Morsilli, M., 2025. Characterization of *Halimeda* bioherms of the Pre-evaporitic messinian of the Salento Peninsula (southern Italy). Sediment. Geol. 475, 106782.

Pastor, F., Valiente, J.A., Palau, J.L., 2019. Sea surface temperature in the Mediterranean: Trends and spatial patterns (1982–2016). In: Meteorol. And Climatol. Of the Mediterranean and Black Seas. Springer, Cham, pp. 297–309.

Pedley, M., Grasso, M., 1994. Upper Miocene peri-Tyrrhenian Reefs in the Calabrian Arc: Sedimentological, tectonic and palaeogeographic implications. Géologie Méditerranéenne 21 (1), 123–136.

Perrin, C., Bosellini, F.R., 2012. Paleobiogeography of scleractinian reef corals: changing patterns during the Oligocene–Miocene climatic transition in the Mediterranean. Earth Sci. Rev. 111 (1–2), 1–24.

Perrin, C., Bosellini, F.R., 2013. The late Miocene coldspot of z-coral diversity in the Mediterranean: patterns and causes. Comptes Rendus Palevol 12, 245–255.

Piller, W.E., Harzhauser, M., 2024. Nubecularia-coralline algal-serpulid-microbial bioherms of the Paratethys Sea—distribution and paleoecological significance (upper Serravallian, upper Sarmatian, Middle Miocene). Geobiology 22, e12590.

Pisera, A., 1996. Miocene reefs of the Paratethys: a review. In: Franseen, E.K., Esteban, M., Ward, W.C., Rouchy, J.M. (Eds.), Models for carbonate stratigraphy, from Miocene reef complex of the Mediterranean regions. Concepts in Sedimentology and Paleontology, volume 5, pp. 97–104. Tulsa, OK.

Plaziat, J.C., Perrin, C., 1992. Multikilometer-sized reefs built by foraminifera (Solenomeris) from the early Eocene of the Pyrenean domain (S. France, N. Spain): Palaeoecologic relations with coral reefs. Palaeogeogr. Palaeoclimatol. Palaeoecol. 96 (3–4), 195–231.

Pomar, L., Bassant, P., Brandano, M., Ruchonnet, C., Janson, X., 2012. Impact of carbonate producing biota on platform architecture: insights from Miocene examples of the Mediterranean region. Earth-Sci. Rev. 113 (3–4), 186–211.

Pomar, L., Hallock, P., 2007. Changes in coral-reef structure through the Miocene in the Mediterranean province: Adaptive versus environmental influence. Geology 35, 899–902.

Pomar, L., Hallock, P., 2008. Carbonate factories: a conundrum in sedimentary geology. Earth Sci. Rev. 87 (3–4), 134–169.

Pomar, L., Baceta, J.I., Hallock, P., Mateu-Vicens, G., Basso, D., 2017. Reef building and carbonate production modes in the west-central Tethys during the Cenozoic. Mar. Pet. Geol. 83, 261–304.

Prista, G.A., Agostinho, R.J., Cachão, M.A., 2015. Observing the past to better understand the future: a synthesis of the Neogene climate in Europe and its perspectives on present climate change. Open Geosci. 7, 20150007.

Reolid, J., Betzler, C., Braga, J.C., Martín, J.M., Lindhorst, S., Reijmer, J.J., 2014. Reef slope geometries and facies distribution: controlling factors (Messinian, SE Spain). Facies 60, 737–753.

Reolid, J., Betzler, C., Braga, J.C., 2016. Amplitude of late Miocene Sea-level fluctuations from karst development in reef-slope deposits (SE Spain). Sediment. Geol. 345, 145–153.

Reolid, J., Betzler, C., Singler, V., Stange, C., Lindhorst, S., 2017a. Facies variability in mixed carbonate–siliciclastic platform slopes (Miocene). Facies 63, 11.

Reolid, J., Betzler, C., Eberli, G.P., Grammer, G.M., 2017b. The importance of microbial binding in Neogene–Quaternary steep slopes. J. Sediment. Res. 87, 567–577.

Reolid, J., Aguirre, J., Pérez-Asensio, J.N., Puga-Bernabéu, Á., Braga, J.C., Martín, J.M., 2022. Mixed carbonate-siliciclastic contourite drift deposits associated with the entrance of an Atlantic-Mediterranean corridor (late Miocene, Southwest Spain). Sediment. Geol. 439, 106233.

Reolid, J., Bialik, O.M., Lindhorst, S., Eisermann, J.O., Petrovic, A., Hincke, C., Beaman, R.J., Webster, J.M., Betzler, C., 2024. A new type of *Halimeda* bioherm on the Queensland Plateau, NE Australia. Coral Reefs 43, 801–821.

Ridgwell, A., Zeebe, R.E., 2005. The role of the global carbonate cycle in the regulation and evolution of the Earth system. Earth Planet. Sci. Lett. 234, 299–315.

Riding, R., Martin, J.M., Braga, J.C., 1991. Coral-stromatolite reef framework, upper Miocene, Almería, Spain. Sedimentology 38, 799–818.

Riedi, M.A., Smith, A.M., 2015. Tube growth and calcification of two reef-building ecosystem engineers in southern New Zealand: *Galeolaria hystrix* and *Spirobranchus cariniferus* (Polychaeta: Serpulidae). Mar. Geol. 367, 212–219.

Robertson, A.H.F., 1977. Tertiary uplift history of the Troodos Massif. Cyprus. Bull. Geol. Soc. Am. 88, 1763–1772.

Robertson, A.H.F., Parlak, O., Ustaömer, T., 2013. Late Palaeozoic–early Cenozoic tectonic development of southern Turkey and the easternmost Mediterranean region: evidence from the inter-relations of continental and oceanic units. In: Robertson, A. H.F., Parlak, O., Ünlügenç, U.C. (Eds.), Geol. Dev. Anatolia and E. Mediterranean Region. Geol. Soc. London, Spec. Publ., 372, pp. 9–48.

Rögl, F., 1999. Mediterranean and Paratethys facts and hypotheses of an Oligocene to Miocene paleogeography (short overview). Geol. Carpath. 50, 339–349.

Rosso, A., Donato, G., Sanfilippo, R., Serio, D., Sciuto, F., D'Alpa, F., Bracchi, V.A., Negri, M.P., Basso, D., 2023. The bryozoan *Margaretta cereoides* as habitat-former in the coralligenous of Marzamemi (SE Sicily, Mediterranean Sea). J. Mar. Sci. Eng. 11, 590.

Rovere, A., Antonioli, F., Bianchi, C.N., 2015. Fixed biological indicators. Handbook of Sea-Level Research 268–280.

Roveri, M., Lugli, S., Manzi, V., 2025. The desiccation and catastrophic refilling of the Mediterranean: 50 years of facts, hypotheses, and myths around the Messinian salinity crisis. Annu. Rev. Mar. Sci. 17 (1), 485–509.

Rusciadelli, G., Sciarra, N., Mangifesta, M., 2003. 2D modelling of large-scale platform margin collapses along an ancient carbonate platform edge (Maiella Mt., Central Apennines, Italy): geological model and conceptual framework. Palaeogeogr. Palaeoclimatol. Palaeoecol. 200, 245–262.

Smith, A.M., 1995. Palaeoenvironmental interpretation using bryozoans: a review. In: Geol. Soc. London, Spec. Publ. 83, 231–243.

Sola, F., Puga-Bernabéu, Á., Aguirre, J., Braga, J.C., 2017. Heterozoan carbonate deposition on a steep basement escarpment (late Miocene, Almería, south-East Spain). Sedimentology 64 (4), 1107–1131.

Sola, F., Braga, J.C., Sælen, G., 2022. Contradictory coeval vertical facies changes in upper Miocene heterozoan carbonate–terrigenous deposits (Sierra de Gádor, Almería, SE Spain). J. Sediment. Res. 92 (3), 257–274.

Syms, C., 2008. Ordination. In: Jørgensen, S.E., Fath, B.D. (Eds.), Encycl. Ecol, Elsevier, Amsterdam, pp. 2572–2581.

Tancredi, S., Margiotta, S., Grasso, S., Tentori, D., Milli, S., 2022. Depositional setting, paleogeography, and sequence stratigraphy of the Salento Peninsula from the Paleogene to the Pleistocene. J. Mediterr. Earth Sci. 14, 47–93.

Tichenor, H.R., Lewis, R.D., 2018. Distribution of encrusting foraminifera at San Salvador, Bahamas: a comparison by reef types and onshore–offshore zonation. J. Foramin. Res. 48, 373–387.

Tomassetti, L., Bosellini, F.R., Brandano, M., 2013. Growth and demise of a Burdigalian coral bioconstruction on a granite rocky substrate (Bonifacio Basin, southeastern Corsica). Facies 59, 703–716.

Tzanova, A., Herbert, T.D., Peterson, L., 2015. Cooling Mediterranean Sea surface temperatures during the late Miocene provide a climate context for evolutionary transitions in Africa and Eurasia. Earth Planet. Sci. Lett. 419, 71–80.

Vaes, B., van Hinsbergen, D.J.J., van de Lagemaat, S.H., van der Wiel, E., Lom, N., Advokaat, E.L., Boschman, L.M., Gallo, L.C., Greve, A., Guilmette, C., Li, S., Lippert, P.C., Montheil, L., Qayyum, A., Langereis, C.G., 2023. A global apparent polar wander path for the last 320 Ma calculated from site-level paleomagnetic data. Earth Sci. Rev. 245, 104547.

Vasiliev, I., Karakitsios, V., Bouloubassi, I., Agiadi, K., Kontakiotis, G., Antonarakou, A., Triantaphyllou, M., Gogou, A., Kafousia, N., de Rafélis, M., Zarkogiannis, S., 2019. Large sea surface temperature, salinity, and productivity–preservation changes preceding the onset of the Messinian Salinity Crisis in the eastern Mediterranean Sea. Paleoceanogr. Paleoclimatol. 34, 182–202.

Verbruggen, H., Kooistra, W.H.C.F., 2004. Morphological characterization of lineages within the calcified tropical seaweed genus *Halimeda* (Bryopsidales, Chlorophyta). Eur. J. Phycol. 39, 213–228.

Veron, J.E.N., Minchin, P.R., 1992. Correlations between sea surface temperature, circulation patterns and the distribution of hermatypic corals of Japan. Cont. Shelf Res. 12, 835–857.

Vescogni, A., Guido, A., 2026. Preservation of Ephemeral Microbial Fabrics: Late Messinian Filamentous Dendrolites from the Salento Peninsula (Central Mediterranean). Palaeogeogr. Palaeoclimatol. Palaeoecol. 113668.

Vescogni, A., Bosellini, F.R., Cipriani, A., Gürler, G., Ilgar, A., Paganelli, E., 2014. The Dağpazarı carbonate platform (Mut Basin, Southern Turkey): Facies and environmental reconstruction of a coral reef system during the Middle Miocene Climatic Optimum. Palaeogeogr. Palaeoclimatol. Palaeoecol. 410, 213–232.

Vescogni, A., Guido, A., Cipriani, A., Gennari, R., Lugli, F., Lugli, S., Manzi, V., Reghizzi, M., Roveri, M., 2022. Palaeoenvironmental setting and depositional model of upper Messinian microbialites of the Salento Peninsula (Southern Italy): A Central Mediterranean Terminal Carbonate complex. Palaeogeogr. Palaeoclimatol. Palaeoecol. 595, 110970.

Vescogni, A., Colombo, F., Guido, A., 2025. New insights into upper Messinian microbial carbonates: A dendrolite–thrombolite build-up from the Salento Peninsula. Central Mediterranean. Geobiology 23, e70023.

Walker, S.E., Parsons-Hubbard, K., Richardson-White, S., Brett, C., Powell, E., 2011. Alpha and beta diversity of encrusting foraminifera that recruit to long-term experiments along a carbonate platform-to-slope gradient: Paleoecological and paleoenvironmental implications. Palaeogeogr. Palaeoclimatol. Palaeoecol. 312, 325–349.

Westerhold, T., Marwan, N., Drury, A.J., Liebrand, D., Agnini, C., Anagnostou, E., Barnet, J.S.K., Bohaty, S.M., De Vleeschouwer, D., Florindo, F., Frederichs, T., Hodell, D.A., Holbourn, A.E., Kroon, D., Lauretano, V., Littler, K., Lourens, L.J., Lyle, M., Pälike, H., Röhl, U., Tian, J., Wilkens, R.H., Wilson, P.A., Zachos, J.C., 2020. An astronomically dated record of Earth's climate and its predictability over the last 66 million years. Science 369, 1383–1387.

Wisshak, M., Rüggeberg, A., 2006. Colonisation and bioerosion of experimental substrates by benthic foraminiferans from euphotic to aphotic depths (Kosterfjord, SW Sweden). Facies 52, 1–17.